

TR-WEL-0005

003

Direction-of-Arrival Estimation of Two Coherent Signals  
Employing the ESPRIT Algorithm for ESPAR Antenna :  
Simulation and Performance Verification

Mickaël Pencolé, Eddy Taillefer ,  
Tomoyuki Aono and Takashi Ohira

2004.10.22

(株)国際電気通信基礎技術研究所  
波動工学研究所

〒619-0288 京都府相楽郡精華町光台二丁目2番地2

Tel: 0774-95-1501 Fax: 0774-95-1508

Advanced Telecommunications Research Institute International  
Wave Engineering Laboratories

2-2-2 Hikaridai, Seika-cho, Soraku-gun, Kyoto 619-0288, Japan

Telephone: +81-774-95-1501 Fax: +81-774-95-1508

©2004 (株)国際電気通信基礎技術研究所

©2004 Advanced Telecommunications Research Institute International



# Contents

<b>Glossary and Key words</b>	<b>vii</b>
<b>Abstract</b>	<b>xi</b>
<b>Introduction</b>	<b>1</b>
<b>1 ATR Wave Engineering Laboratories</b>	<b>3</b>
1.1 Introduction to ATR . . . . .	3
1.2 Wave Engineering Laboratories . . . . .	4
<b>2 Objective and Background</b>	<b>7</b>
2.1 Main Objective . . . . .	7
2.2 Techniques of DoA Estimation . . . . .	7
2.3 The New Approach . . . . .	8
2.4 Synopsis of Work . . . . .	9
<b>3 The ESPAR Antenna and its Applications</b>	<b>11</b>
3.1 The Configuration of the 7-element ESPAR Antenna . . . . .	11
3.2 The Signal Model of the 7-element ESPAR Antenna . . . . .	14
3.3 Applications of the ESPAR Antenna . . . . .	15
3.3.1 Wireless Ad-Hoc Community Network . . . . .	15
3.3.2 Anti-Eavesdrop Secret Key for Wireless Communications	16
3.3.3 Terrestrial Digital TV . . . . .	17
<b>4 The ESPRIT Algorithm Principle for ESPAR Antennas</b>	<b>19</b>
4.1 ESPRIT Algorithm for ESPAR Antenna . . . . .	19
4.2 Coherent Signals . . . . .	22
4.3 Simulation Results with Two Highly Correlated Signals . . . . .	23
4.3.1 Simulation protocol . . . . .	23
4.3.2 Influence of the correlation coefficient $\rho$ and SNR value on the DoA estimation performance . . . . .	24
4.3.3 Angular variation influence on DoA estimation . . . . .	26

<b>5 The ESPRIT Algorithm for ESPAR Antennas Combined with Forward-Backward Averaging Technique</b>	<b>29</b>
5.1 Forward-Backward Averaging Technique Combined with the ESPRIT Algorithm for ESPAR Antenna . . . . .	29
5.2 Simulation Results of DoA Estimation Employing FBA-ESPRIT Algorithm for ESPAR Antenna . . . . .	31
<b>Conclusion</b>	<b>35</b>
<b>Acknowledgements</b>	<b>37</b>
<b>References</b>	<b>41</b>
<b>Appendix A : MatLab Source Codes</b>	<b>43</b>
creer_2sigcorr.m . . . . .	43
esprit_sans_fb.m . . . . .	45
esprit_avec_fb.m . . . . .	47
cal_w.m . . . . .	49
<b>Appendix B : Influence of Correlation Coefficient <math>\rho</math>, SNR and Angular Distance Between Signals on DoA Estimation</b>	<b>51</b>
esprit_var_rho.m . . . . .	51
esprit_var_SNR.m . . . . .	58
esprit_var_angle.m . . . . .	65

# List of Figures

1.1	Organization of ATR . . . . .	4
1.2	Organization of Wave Engineering Laboratories . . . . .	5
3.1	7-element adaptive ESPAR antenna . . . . .	12
3.2	Internal structure of the ESPAR antenna . . . . .	13
3.3	Architecture of conventional and ESPAR array antennas . . . . .	13
3.4	Top view of the 7-element adaptive ESPAR antenna . . . . .	14
3.5	WACNet: example of routing . . . . .	15
3.6	Transmitting the secret key on air, it may be eavesdropped . . . . .	17
3.7	Novel idea for secret key agreement . . . . .	17
3.8	Receiving power . . . . .	18
4.1	Displacement invariance. . . . .	20
4.2	Reactance-domain technique. . . . .	20
4.3	Influence of SNR on DoA estimation performance for two uncorrelated and highly correlated signals. The DoAs are $\theta_1 = 35^\circ$ ; $\theta_2 = 145^\circ$ . . . . .	24
4.4	Influence of the correlation coefficient on DoA estimation performance. DoAs are $\theta_1 = 35^\circ$ , $\theta_2 = 145^\circ$ , $SNR = 25$ dB, 2 000 trial runs. . . . .	25
4.5	Variation in angular difference between signals. . . . .	26
4.6	Influence of angular variation in DoA estimation error ( $\epsilon$ ) for coherent signals, with an angular distance of $\Delta\theta$ between the two signals; $\rho$ denotes the correlation coefficient between the two signals, $SNR=25$ dB. . . . .	27
5.1	Reordering of the elements of the antennas. . . . .	30
5.2	Effect of FBA on decorrelation of two coherent signals in a noise-free environment ( $SNR = \infty$ ). The DoAs are $\theta_1 = 35^\circ$ , $\theta_2 = 145^\circ$ ; 2 000 independent trial runs. . . . .	32
5.3	Effect of SNR on DoA estimation. The DoAs are $\theta_1 = 35^\circ$ , $\theta_2 = 145^\circ$ ; 2 000 independent trial runs. . . . .	32

5.4	Effect of FBA on ESPRIT for ESPAR for two coherent signals with angular distance $\Delta\theta =  \theta_2 - \theta_1 $ (SNR=40 dB; correlation coefficient $\rho = 0.9997$ , 2 000 independent trial runs). . . . .	33
5.5	Scatter of phase factors $\phi_1$ and $\phi_2$ for two coherent signals with correlation coefficient $\rho$ , employing ESPRIT for ESPAR(5.5(a), 5.5(c) and 5.5(e)) and FBA-ESPRIT for ESPAR(5.5(b), 5.5(d) and 5.5(f)). SNR=25 dB, 300 trial runs (except for: 5.5(e) and 5.5(f): 50 trial runs). . . . .	34

# List of Tables

2.1	Internship progress and schedule . . . . .	10
-----	--	----





# GLOSSARY AND KEY WORDS

## Glossary

**A/D:** Analog to Digital

**AP:** Antennas and Propagation

**ATR:** Advanced Telecommunications Research

**CUBA:** Circular Uniform Beam Arrays

**DoA:** Direction-of-Arrival

**ESPAR:** Electronically Steerable Parasitic Array Radiator

**ESPRIT:** Estimation of Signal Parameters via Rotational Invariance Techniques

**FBA:** Forward-Backward Averaging

**FFT:** Fast Fourier Transform

**IEEE:** Institute of Electrical and Electronics Engineers

**IEICE:** Institute of Electronics, Information and Communication Engineers

**LED:** Light Emitting Diode

**MUSIC:** Multiple Signal Classification

**PPCC:** Power Pattern Cross Correlation

**R&D:** Research and Development

**RCS:** Radio Communication Systems

**RF:** Radio Frequency

**SAGE:** Space Alternating Generalized Expectation maximization

**SINR:** Signal to Interference Noise Ratio

**SNR:** Signal to Noise Ratio

**SSP:** Spatial Smoothing Preprocessing

**TLS:** Total Least Squares

**TV:** TeleVision

**WACNet:** Wireless Ad-hoc Community Network

## Key words

ESPAR Antenna, Direction-of-Arrival Estimation, ESPRIT Algorithm, Forward-Backward Averaging Technique, Coherent Signals, Correlation Coefficient, Translational Invariance, Reactance, Array Antenna, Signal Processing.

# NOTATIONS

In this report, the following mathematical notations will be used for equations and calculus:

$a, A$  denote a scalar or a complex value,

$\mathbf{a}$  denotes a vector,

$\mathbf{A}$  is a matrix,

$\mathbf{A}^T$  represents the transpose operation for the matrix  $\mathbf{A}$ ,

$\mathbf{A}^{-1}$  represents the inverse for the matrix  $\mathbf{A}$ ,

$\mathbf{A}^H$  represents the hermitian for the matrix  $\mathbf{A}$ ,

$\mathbf{A}^*$  represents the conjugate for the matrix  $\mathbf{A}$ ,

$E[\cdot]$  is the expectation operator,

$|a|$  represents the norm of  $a$ ,

$\Re(a)$  represents the real part of the complex  $a$ ,

$\Im(a)$  represents the imaginary part of the complex  $a$ ,

$\hat{a}$  and  $\hat{\mathbf{A}}$  represent the estimate of the value of  $a$  and  $\mathbf{A}$ , respectively.



# ABSTRACT

The Electronically Steerable Parasitic Array Radiator (ESPAR) antenna is a single output adaptive antenna that offers low cost and low complexity relative to conventional array antennas. A method to estimate direction of arrival (DoA) based on the ESPRIT algorithm has been proposed for a particular 7-element regular hexagonal shaped ESPAR antenna. Nevertheless, this algorithm has never been applied with coherent signals. Therefore, simulations are conducted to investigate the performance of the ESPRIT algorithm for ESPAR antenna in the case of coherent waves. Results show that the DoA estimation performance decreases as the correlation coefficient increases.

In this report, a method to apply the forward-backward averaging (FBA) technique with the ESPRIT algorithm for ESPAR antenna is proposed to improve performance in the case of coherent signals. Simulations show that, in a noise-free environment, the FBA technique can perfectly resolve<sup>1</sup> coherent signals. In a low-noise environment, the proposed technique can improve the accuracy of the ESPAR antenna of about 5°. In the noisy case, the FBA technique does not give a worse performance than the original ESPRIT algorithm for ESPAR antenna. Moreover, the FBA technique provides a criterion for the reliability of the estimates based on the unit-circle. Finally, using the new technique, the computational complexity of the algorithm is not increased. Thus, the proposed method is an improved version of the ESPRIT algorithm for ESPAR antenna.

---

<sup>1</sup>In this report, “resolve” refers to the capability of a parameter estimation method to yield estimates with different arguments for distinct signals.



# INTRODUCTION

With the development of wireless communications, adaptive array antennas are a subject of great research interest due to its ability to improve the performance of wireless systems. These antennas can form beams towards desired users and nulls towards interferers simultaneously. However, traditional smart antennas requires complex base-band digital signal processors, A/D converters for each element, what implies a high power consumption.

The Wave Engineering Laboratories are conducting research on Electronically Steerable Parasitic Array Radiator (ESPAR) antennas. Those analog adaptive array antennas provides a dramatically simplified architecture that results in significantly lower power dissipation and fabrication cost than are common with digital beamforming antennas. The ESPAR antenna offers different services such as the interference reduction, the mitigation of multipath fading by angle diversity effect or direction of arrival (DoA) estimation.

Recently, the ESPRIT algorithm for ESPAR antenna was presented for DoA estimation. This algorithm achieves a significant reduction in computational complexity over previous algorithms such as MUSIC [7] by exploiting the displacement invariance structure of the ESPAR antenna. Simulations have shown that the ESPRIT algorithm for ESPAR antenna can correctly estimate DoA of uncorrelated signals. However, this algorithm was not adapted to estimate the DoA of coherent signals, and DoA estimation simulations have been performed only in the case of incoherent signals.

The purpose of this report is to investigate the effect of coherent signals on the DoA estimation performance employing the ESPRIT algorithm for ESPAR antenna. This report also proposes a technique to improve DoA estimation of coherent signals by combining the forward-backward averaging (FBA) technique with the ESPRIT algorithm for ESPAR antenna.

After introducing the ESPAR antenna's features, some applications of the antenna will be presented. A review of the ESPRIT algorithm for ESPAR antenna (ESPRIT for ESPAR) is then proposed. Some simulations are also conducted to evaluate the DoA estimation function of the correlation coefficient  $\rho$ . Then, a method to combine the FBA technique with the ES-

PRIT algorithm for ESPAR antenna is proposed. Finally, some simulations compare the performance of ESPRIT for ESPAR with ESPRIT for ESPAR combined with the FBA technique in the case of coherent signals.



# Chapter 1

## ATR Wave Engineering Laboratories

### 1.1 Introduction to ATR

Advanced Telecommunications Research Institute International<sup>1</sup> (ATR) was established in 1986 with support from different sections of industry, academia and government. ATR is an independent corporation which conducts R&D, both basic and advanced, in the field of telecommunications. Its policy is to:

- promote basic and creative telecommunications research,
- joint research opportunities for industrial, academic and governmental organisations,
- contribute to international society,
- play a central role in Kansai Science City.

Research is commissioned by public and private sectors, or carried out with funds obtained through open competition. In 2004, the research funding system was shifted from a governmental organisation called TAO (Telecommunication Advancement Organization of Japan) to NICT (National institute of Information Communications of Japan) that results from the merger of CRL (Communications Research Laboratory) and TAO. In June 2003, the capital of ATR was approximately of ¥22 billion.

The recent reorganized structure of ATR leads to the eight following laboratories: SLT, ACR, WEL, HIS, NIS, CNS, MIS and IRC, as shown in

---

<sup>1</sup><http://www.atr.jp>

Figure 1.1.

In April 2004, 390 employees worked in ATR, among them 329 were

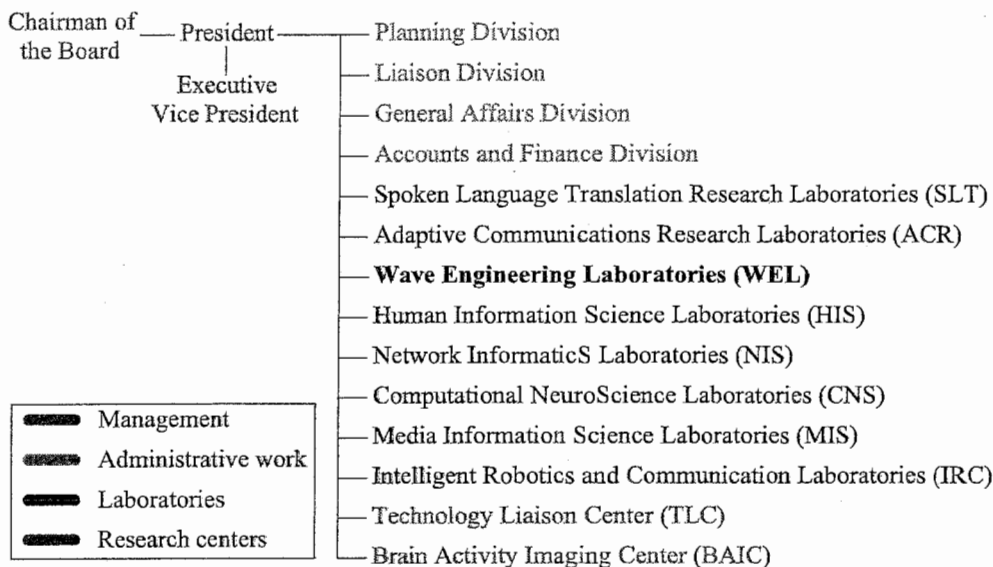


FIGURE 1.1: Organization of ATR

researchers. ATR is a research institute that has established relationships both domestically and abroad.

## 1.2 Wave Engineering Laboratories

The Wave Engineering Laboratories (WEL) were created in April 2004. They result from the division of the former ACR laboratories. Departments 1 and 2 of the ex-ACR laboratories form the actual ACR laboratories rather than Departments 3 and 4 represent the Wave Engineering Laboratories.

The aim of WEL is to develop innovative antennas and devices for wireless communications. It is divided into three departments as depicted in Figure 1.2.

Within the department of Radio Waves, research is being carried out on smart antennas, promising key components for future wireless ad-hoc networks. The four main research domains of the department of Radio Waves are the adaptive wireless system devices, security in wireless systems (secret key), direction-of-arrival (DoA) detection and the antenna design.

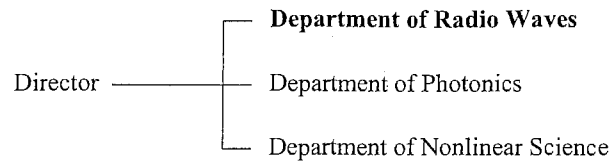


FIGURE 1.2: Organization of Wave Engineering Laboratories

I performed my internship within the Wave Engineering Laboratories in the DoA detection group during a period of six months. The content of my work is described in the following of this report.



## Chapter 2

# Objective and Background

### 2.1 Main Objective

The ESPAR antenna is a kind of adaptive array antenna that offers several impressive functionalities, including programmable control of antenna radiation-pattern, direction-of-arrival (DoA) estimation, and adaptive steering of its beam and nulls to enhance the signal-to-interference-noise ratio (SINR). Recently, the ESPRIT algorithm for ESPAR antenna was presented for DoA estimation [4]. However, DoA estimation simulations with ESPRIT algorithm for ESPAR have been performed only in the case of non-coherent waves. First, simulations are presented to inspect the DoA estimation performance of coherent signals employing the ESPRIT algorithm for ESPAR antenna. Then, a method that can decorrelate coherent signals combining the forward-backward averaging technique with the standard ESPRIT algorithm for ESPAR antenna is proposed.

### 2.2 Techniques of DoA Estimation

Direction-of-arrival estimation is a prior step to any adaptive control of the antenna. Concerning this topic, different techniques have been applied to the ESPAR antenna.

The first technique used with ESPAR antenna consists of a radio-wave detector that points out the angle for which the received signal has the maximum amplitude [12]. Twelve narrow beams are formed and steered in  $0^\circ$  to  $360^\circ$  angles by step of  $30^\circ$ . Thus, there is a direct correspondance between the beams and the angles.  $30^\circ$  is the lowest bound that make possible to differentiate two adjacent beams. For each beam, the ESPAR antenna detects the received signal strength while the wave is arriving. Finally, the angle

corresponding to the beam of maximum strength is searched and therefore, indicated with one of the twelve LEDs.

The second technique applied to the ESPAR antenna was the MUSIC algorithm. This algorithm provides asymptotically unbiased estimates of the characteristics of incident signals, like the DoAs, strengths and cross correlations among the incident waveforms and noise/interference strength [17].

A third technique of DoA estimation based on cross-correlation between the antenna output and radiation pattern called PPCC was also proposed [22]. To estimate the DoA  $\theta$  of a signal impinging on the antenna,  $N$  different sets of reactance are chosen so as to obtain  $N$  antenna power patterns. The estimated angle  $\hat{\theta}$  is then determined, using the fact that the correlation coefficient between the output power of the antenna of each corresponding reactance vector and the antenna power pattern is the highest at angle  $\hat{\theta}$ .

A technique called CUBA-MUSIC was also proposed to estimate DoA with the ESPAR antenna [11]. The CUBA-MUSIC algorithm is based on FFT of reactance-domain output signal. Thanks to six patterns and a transformation of the output signal, properties of a linear antenna can be obtained for the 7-element ESPAR antenna in order to employ the MUSIC algorithm.

The SAGE algorithm was adapted to the ESPAR antenna in order to estimate signal direction-of-arrivals and delays [10]. The SAGE algorithm adopts a maximum-likelihood approach, i.e., it aims at maximizing some likelihood functions to estimate the unknown parameters.

The ESPRIT algorithm was adapted to the ESPAR antenna [4] to achieve DoA estimations. This technique is a subspace-based approach for source parameter estimation for planar wavefronts. To estimate DoA, the ESPRIT algorithm requires a translational invariance within the antenna structure. This algorithm also uses as a pre-processing the reactance domain technique to calculate a suitable correlation matrix [8].

## 2.3 The New Approach

The ESPRIT algorithm has successfully been applied to the ESPAR antenna and could estimate up to 3 uncorrelated signals. In the case of coherent signals, a degradation of DoA estimation performance can be observed. To improve the DoA estimation performance in the case of low-noise environment, the forward-backward averaging technique combined with the ESPRIT algorithm for ESPAR antenna is proposed in this report. The benefit of this technique is that it can decorrelate coherent or highly correlated signals [1]. The FBA technique has already been applied in the case of the

reactance-domain SSP MUSIC for the ESPAR antenna [7].

## 2.4 Synopsis of Work

Period	Work contents	Comments
April	<b>Documentation work:</b> <ul style="list-style-type: none"> <li>• The ESPAR antenna features</li> <li>• The conventional ESPRIT algorithm</li> <li>• The FBA technique</li> </ul>	Study of former articles concerning the ESPAR antenna and the ESPRIT algorithm [3, 20, 18, 4, 6, 1, 7, 2].
May to June	<b>Investigation of the influence of three main parameters on the DoA estimation performance of the ESPRIT algorithm for ESPAR antenna:</b> <ul style="list-style-type: none"> <li>• Correlation coefficient <math>\rho</math> between signals</li> <li>• SNR (dB)</li> <li>• Angular difference between signals</li> </ul>	The ESPRIT algorithm for ESPAR antenna was applied to coherent signals for the first time.
<i>Continue in next page...</i>		

Period	Work contents	Comments
June to July	<p>Forward-backward averaging technique applied to ESPRIT algorithm for ESPAR antenna:</p> <ul style="list-style-type: none"> <li>• Implementation of FBA technique with ESPRIT algorithm for ESPAR antenna</li> <li>• Simulations: DoA estimation of two coherent signals employing the FBA-ESPRIT algorithm</li> </ul>	The FBA technique has been successfully applied to the ESPRIT algorithm for ESPAR antenna.
July to August	<p>Writing papers for national conference:</p> <p>IEICE, General Conference, Tokushima, September, 21<sup>st</sup> [14].</p> <p>IEICE, RCS AP, Niigata, October, 29<sup>th</sup> [13].</p>	
September	<p>Preparation of the oral presentation</p> <p>Documentation work for the next part of the research topic</p>	

Table 2.1: Internship progress and schedule



## Chapter 3

# The ESPAR Antenna and its Applications

In this chapter, the configuration of the 7-element ESPAR (Electronically Steerable Parasitic Array Radiator) antenna is introduced. Then, the signal model used for this antenna is detailed. In Sec. 3.3, some applications of this antenna are described.

### 3.1 The Configuration of the 7-element ESPAR Antenna

The ESPAR antenna is a single quarter-wavelength ( $\lambda/4$ ) vertical monopole radiator #0 on a ground plane surrounded by  $M$  parasitic monopole elements [3]. Fig. 3.1 shows the geometry of an  $M + 1$ -element ESPAR antenna with  $M = 6$ . The central element itself exhibits an omni-directional radiation pattern. To establish directivity by electronics means, each parasitic element # $m$  is loaded with varactors having reactance  $x_m$  ( $m = 1, 2, \dots, M$ ). The patterns of the antenna can be changed by adjusting the values of these reactances. The vector denoted by  $\mathbf{x} = [x_1, x_2, \dots, x_M]$  is called the reactance vector.

The ESPAR antenna can run as well in a receive mode as in a transmit mode. For convenience, the model of the ESPAR antenna is derived in a transmit mode. However, according to the theorem of reciprocity, the receive mode radiation pattern of an antenna is equal to that of the transmit mode. To formulate the behavior of the ESPAR antenna, the analog RF-current and RF-voltage vectors are defined by:

$$\mathbf{i} = \mathbf{Y}\mathbf{v}, \mathbf{i} = [i_0, i_1, \dots, i_M]^T, \mathbf{v} = [v_0, v_1, \dots, v_M]^T, \quad (3.1)$$

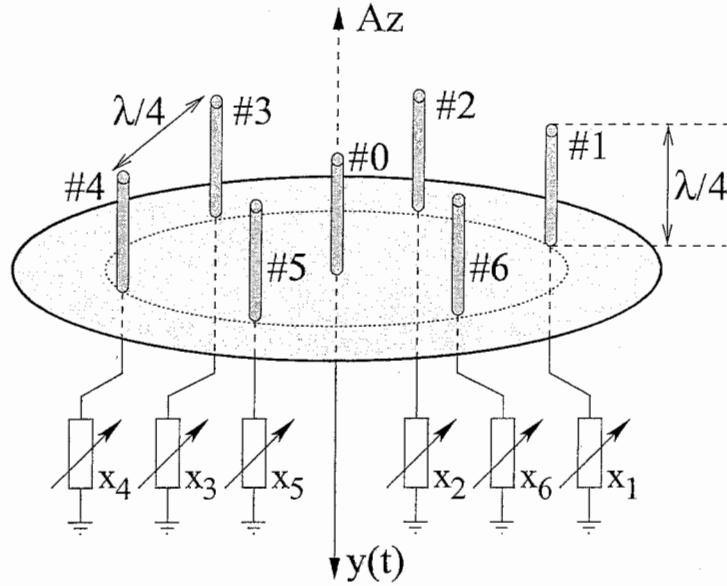


FIGURE 3.1: 7-element adaptive ESPAR antenna

where  $i_m$  and  $v_m$  represent the RF-current and the RF-voltage associated to the  $m^{\text{th}}$  element ( $m = 0, 1, \dots, M$ ), as shown in Fig. 3.2.  $\mathbf{Y}$  represents the admittance matrix and it involves mutual coupling among elements. In the particular case of the 7-element ESPAR antenna, the admittance matrix  $\mathbf{Y}$  is expressed as:

$$\mathbf{Y} = \begin{bmatrix} y_{00} & y_{01} & y_{01} & y_{01} & y_{01} & y_{01} & y_{01} \\ y_{01} & y_{11} & y_{12} & y_{13} & y_{14} & y_{13} & y_{12} \\ y_{01} & y_{12} & y_{11} & \ddots & \ddots & \ddots & y_{13} \\ y_{01} & y_{13} & \ddots & y_{11} & \ddots & \ddots & y_{14} \\ y_{01} & y_{14} & \ddots & \ddots & y_{11} & \ddots & y_{13} \\ y_{01} & y_{13} & \ddots & \ddots & \ddots & y_{11} & y_{12} \\ y_{01} & y_{12} & y_{13} & y_{14} & y_{13} & y_{12} & y_{11} \end{bmatrix}. \quad (3.2)$$

The components of the matrix  $\mathbf{Y}$  have these physical meanings due to the circular symmetry of the ESPAR antenna:

- $y_{00}$  : center radiator's self admittance,
- $y_{01}$  : mutual admittance between center and parasite,
- $y_{11}$  : parasite's self admittance,
- $y_{1k}$  : mutual admittance between parasites.

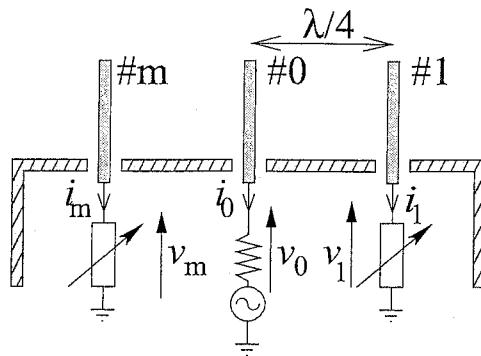


FIGURE 3.2: Internal structure of the ESPAR antenna

For the 7-element ESPAR antenna, the number of independent components is equal to 6.

Compared with conventional array antennas (Fig. 3.3(a)), ESPAR antenna has low hardware complexity, low cost and low power consumption. Indeed, due to its single fed output, the ESPAR antenna does not need RF-amplifiers, bandpass filters, A/D converters for each element like in conventional adaptive array, as shown in Fig. 3.3(b).

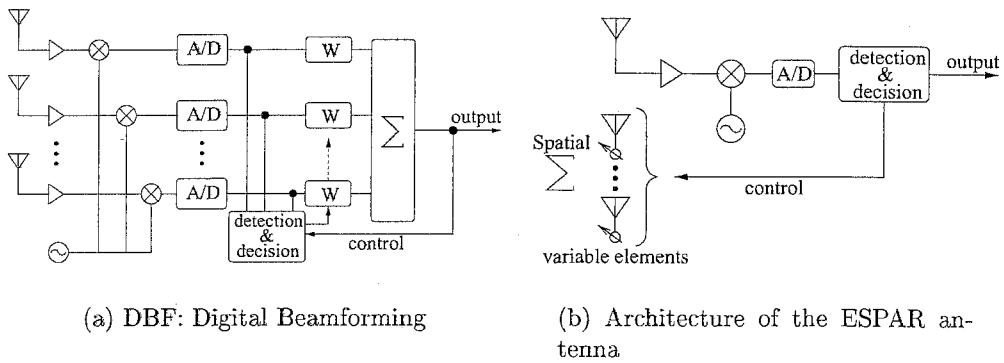


FIGURE 3.3: Architecture of conventional and ESPAR array antennas

### 3.2 The Signal Model of the 7-element ESPAR Antenna

Analogously to conventional phased arrays, the steering vector and the weight vector of the ESPAR antenna play a key role to calculate the radiation directivity. In the case of a reception with  $Q$  signals impinging on the ESPAR antenna, the matrix  $\mathbf{A}$  containing all the steering vectors  $\mathbf{a}(\theta_q)$  ( $q = 1, \dots, Q$ ) is expressed as:

$$\mathbf{A} = [\mathbf{a}(\theta_1), \dots, \mathbf{a}(\theta_q), \dots, \mathbf{a}(\theta_Q)]. \quad (3.3)$$

The steering vector  $\mathbf{a}(\theta_q)$ , depending on the structure of the ESPAR antenna for the  $q^{\text{th}}$  signal, is expressed as:

$$\mathbf{a}(\theta_q) = \begin{bmatrix} 1 \\ e^{j\frac{\pi}{2} \cos(\theta_q - \varphi_1)} \\ e^{j\frac{\pi}{2} \cos(\theta_q - \varphi_2)} \\ \vdots \\ e^{j\frac{\pi}{2} \cos(\theta_q - \varphi_M)} \end{bmatrix}, \quad (3.4)$$

where  $\varphi_m = \frac{2\pi}{M}(m-1)$ , ( $m = 1, \dots, M$ ) represents the value of the angle between the azimuthal reference and the  $m^{\text{th}}$  parasitic element, as shown in Fig. 3.4. The RF equivalent weight vector  $\mathbf{w}$  is considered equivalent to the

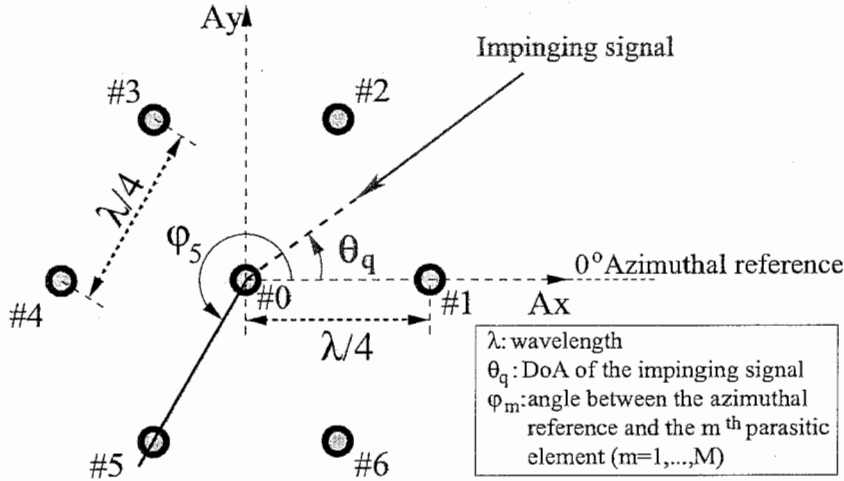


FIGURE 3.4: Top view of the 7-element adaptive ESPAR antenna

current vector  $\mathbf{i}$  and is given by:

$$\mathbf{w} = 2z_s(\mathbf{Z} + \mathbf{X})^{-1}\mathbf{u}_0, \quad (3.5)$$

where  $\mathbf{X} = \text{diag}\{z_s, jx_1, jx_2, \dots, jx_M\}$  is the reactance matrix,  $\mathbf{Z}$  is the impedance matrix,  $z_s = 50 \Omega$  is the receiver input impedance, and the  $M + 1$  dimensional vector  $u_0$  is equal to  $[1, 0, \dots, 0]^T$ . If  $Q$  waves having the signal form  $\mathbf{s}(t) = [s_1(t), s_2(t), \dots, s_Q(t)]^T$  arrive simultaneously at the ESPAR antenna, the output signal model is given by

$$y(t) = \mathbf{w}^T \sum_{q=1}^Q \mathbf{a}(\theta_q) s_q(t) + n(t) \quad (3.6)$$

$$= \mathbf{w}^T \mathbf{A} \mathbf{s}(t) + n(t), \quad (3.7)$$

where  $n(t)$  is an additive white Gaussian noise.

### 3.3 Applications of the ESPAR Antenna

The whole and the diversity of the functionalities that the ESPAR antenna can offer allow to use it in various applications as the WACNet, the Anti-Eavesdrop Secret Key for Wireless Communications or in applications for Terrestrial Digital TV.

#### 3.3.1 Wireless Ad-Hoc Community Network

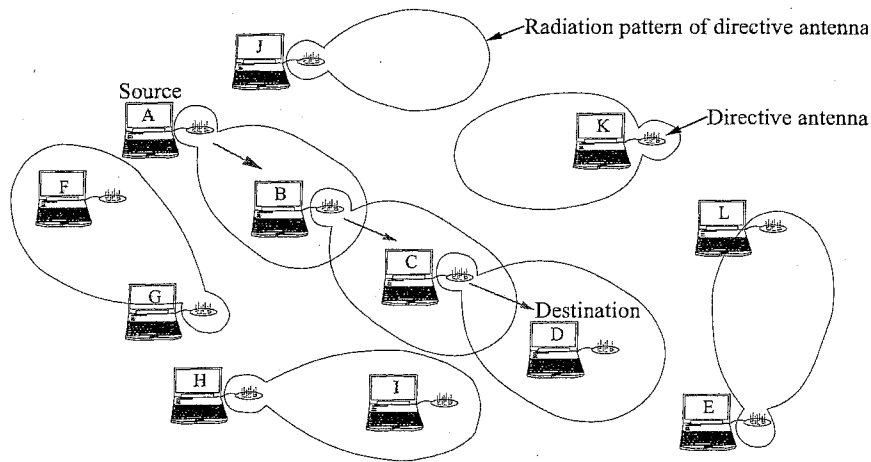


FIGURE 3.5: WACNet: example of routing

The Wireless Ad-Hoc Community Networks (WACNet) [5] can be considered as a means of communication among portable user terminals that

temporally meet, where distance and time come close yet easy connection to a network infrastructure is not possible. This concept of WACNet has been proposed in order to have more scalability, more speeds, and low output power level over previous techniques that enable wireless ad-hoc networks, such as Bluetooth.

The WACNet consists of portable user terminals and has no infrastructure such as hosts, base stations, switches, and hubs. It is therefore expected to be applicable anywhere; not only in fixed space such as an office company, but also in a moving space such as a train. The WACNet has scalability, i.e., the ability to accept a large number of users terminals because of autonomous segmentation and routing (Fig. 3.5).

### **3.3.2 Anti-Eavesdrop Secret Key for Wireless Communications**

As wireless communication systems such as wireless LANs are experiencing explosive growth, the security of them has become a critical issue. The concern about privacy protection and the securities of industrial secrets has been growing up. To prevent secret information from being eavesdropped, the communication contents may be encrypted thanks to secret keys, such as id numbers or passwords. If the secret keys are eavesdropped in the process of transmitting on air, all encrypted information after that shall be decrypted. The weak point of conventional systems lie in distribution of secret key information by radio waves.

With the ESPAR antenna, a key agreement without distribution can be obtained. The idea is based on a variable directional antenna (ESPAR) and the reciprocity theorem of radio wave propagation. First of all, constant amplitude radio waves are transmitted from the access point (the variable directional antenna) to the user terminal with varying beam pattern using a variable directional antenna. Soon after, the user terminal transmits constant amplitude radio waves back to the access point. Thanks to the reciprocity theorem of radio wave propagation between uplink and downlink, the strength of the signals received by the user terminal and the access point are proportional to each other. Thus, because the characteristics of radio transmission depend on the unique combination of antenna performances and positions of a pair of transmitters and receivers, the keys generated by eavesdroppers are not the same as the keys generated by the access point and the user terminal. The ESPAR antenna is suitable to consumer products because it consists of simple circuits and has a low fabrication cost.

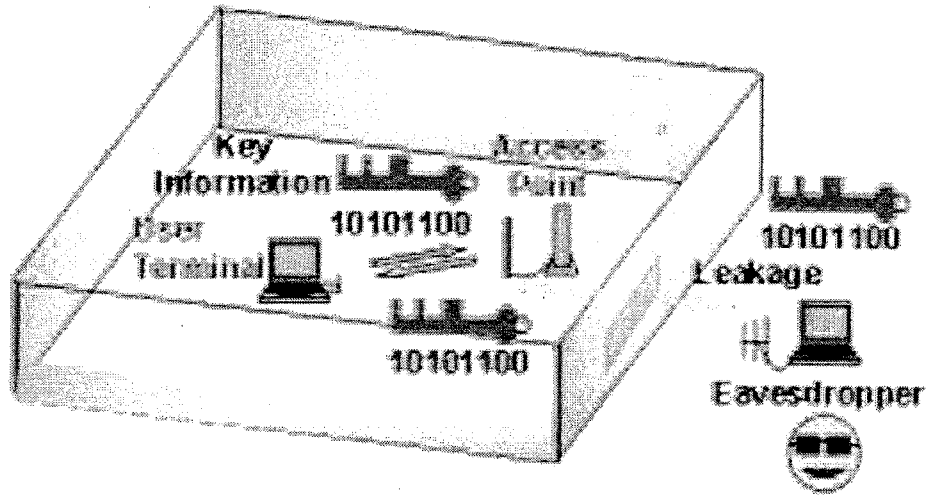


FIGURE 3.6: Transmitting the secret key on air, it may be eavesdropped

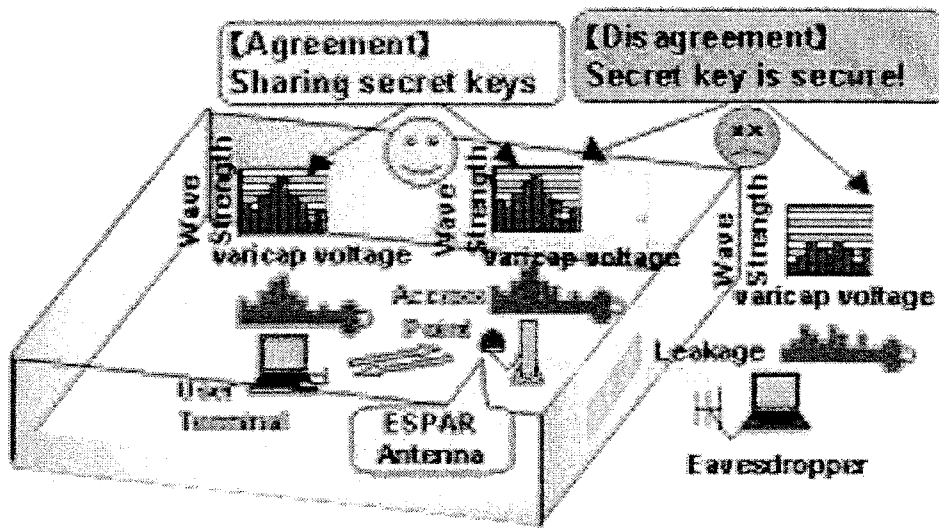


FIGURE 3.7: Novel idea for secret key agreement

### 3.3.3 Terrestrial Digital TV

The ESPAR antenna can be used to receive terrestrial digital television broadcasting. Because the rotation angle changes due to movement of per-

sons and channel, antenna rotation must be adjusted whenever pictures are not received. Contrary to standard antennas, the ESPAR antenna can keep above a marginal level the receiving power, changing automatically the directivity of the antenna. By this way, in the case of indoor reception, pictures can be received with one fourth broadcasting power. This implies that, using the ESPAR antenna, pictures can be received at a location where is 2 times farer away from the broadcast transmitting station.

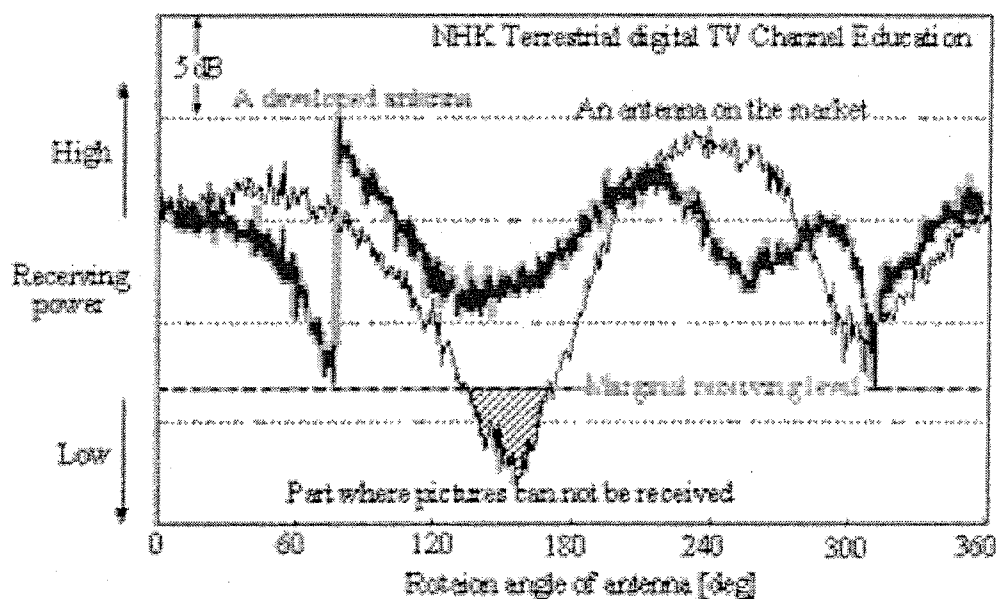


FIGURE 3.8: Receiving power



## Chapter 4

# The ESPRIT Algorithm Principle for ESPAR Antennas

The ESPRIT algorithm [18] is a high-resolution signal parameter estimation technique based on the translational invariance structure of a sensor array. This algorithm achieves a significant reduction in computational complexity over previous algorithms such as MUSIC. In this chapter, a review of the ESPRIT algorithm for ESPAR antenna [4] is proposed. Simulation results carried out with two highly correlated signals are also presented to estimate the performance of this algorithm.

### 4.1 ESPRIT Algorithm for ESPAR Antenna

Recently, the ESPRIT algorithm for ESPAR antenna was presented for Direction-of-Arrival (DoA) estimation [4]. To apply the ESPRIT algorithm, the geometric structure of the antenna must present a translational invariance. The 7-element ESPAR antenna fits this criterion thanks to its specific design with a regular hexagonal shape [21]. Indeed, two subarrays (Fig. 4.1) with the same sensitivity pattern are found in the 7-element ESPAR antenna's geometry, separated by a constant vector  $\vec{\Delta}$  (also called the displacement vector) [18].

Due to the single-port output of the ESPAR antenna, a correlation matrix on element outputs cannot be directly computed. However, by employing the reactance-domain technique [17], a correlation matrix  $\mathbf{R}_{yy}$  can be computed. This technique consists of measuring  $M + 1$  outputs  $y_m(t_m)$ , ( $m = 1, \dots, M + 1$ ) for  $M + 1$  different sets of reactances  $\{\mathbf{x}_{(1)}, \dots, \mathbf{x}_{(M+1)}\}$ , by sending  $M + 1$  times the same signal (see Fig. 4.2). The obtained output vector  $\mathbf{y}$  is represented in Fig. 4.2, with  $t_2 = t_1 + KT$ , where  $K$  represents

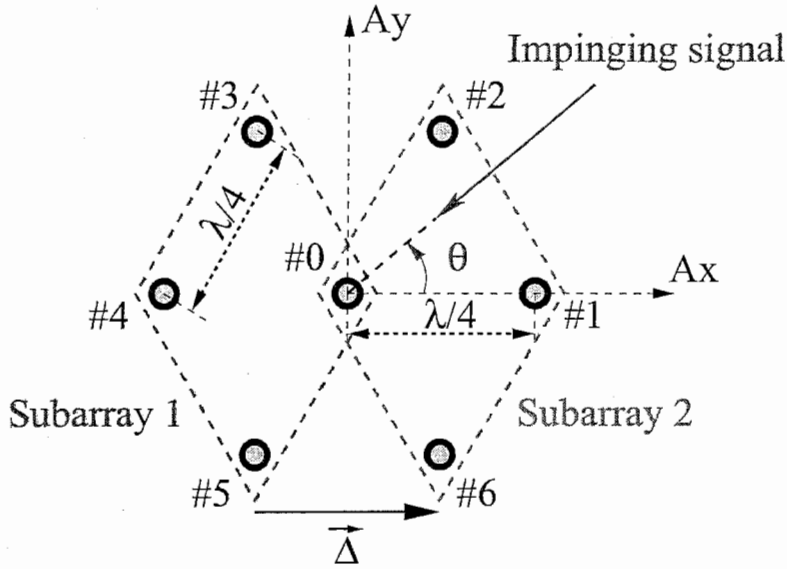


FIGURE 4.1: Displacement invariance.

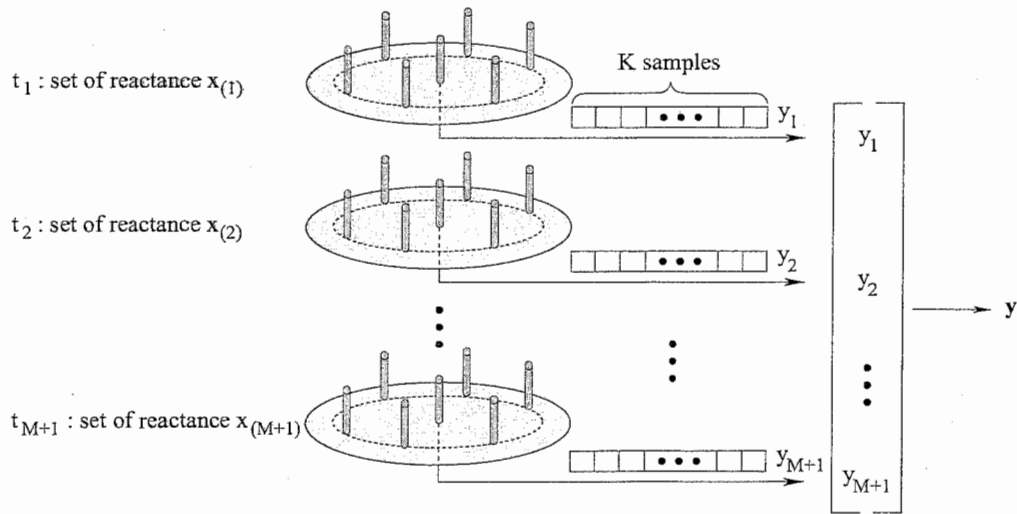


FIGURE 4.2: Reactance-domain technique.

the number of samples and  $\frac{1}{T}$  is the sampling frequency.

Then, the vector  $\mathbf{y} = [y_1(t_1), \dots, y_{M+1}(t_{M+1})]^T$  allows us to compute the correlation matrix:

$$\mathbf{R}_{\mathbf{y}\mathbf{y}} = E[\mathbf{y}\mathbf{y}^H]. \quad (4.1)$$

Using the ESPAR antenna output signal model (3.7), the reactance-domain correlation matrix is expressed as

$$E[\mathbf{y}\mathbf{y}^H] = \mathbf{W}^T \mathbf{A} \mathbf{R}_{ss} \mathbf{A}^H \mathbf{W}^* + \mathbf{R}_{nn}, \quad (4.2)$$

where  $\mathbf{W} = [\mathbf{w}_{(1)}, \dots, \mathbf{w}_{(M+1)}]$  represents the weight matrix corresponding to the measured output vector,  $\mathbf{R}_{ss} = E[\mathbf{s}\mathbf{s}^H]$ , where  $\mathbf{s}$  is defined in Sec. 3.2, and  $\mathbf{R}_{nn}$  is the noise covariance matrix. Nevertheless, in our simulations, the matrix  $\mathbf{R}_{yy}$  is estimated as follows:

$$\hat{\mathbf{R}}_{yy} = \frac{1}{K} \sum_{k=1}^K \begin{bmatrix} y_1[k] \\ y_2[k] \\ \vdots \\ y_{M+1}[k] \end{bmatrix} \begin{bmatrix} y_1[k]^* & y_2[k]^* & \cdots & y_{M+1}[k]^* \end{bmatrix}. \quad (4.3)$$

However, this reactance-domain correlation matrix cannot be used directly with the ESPRIT algorithm. Therefore, a modified correlation matrix  $\mathbf{R}_{xx}$  is used:

$$\mathbf{R}_{xx} = (\mathbf{W}^T)^{-1} (\mathbf{R}_{yy} - \hat{\mathbf{R}}_{nn}) (\mathbf{W}^*)^{-1}, \quad (4.4)$$

where  $\hat{\mathbf{R}}_{nn}$  is an estimate of the noise covariance matrix given by the Akaike's information criterion (AIC) [23] and  $\mathbf{W}$  is a constant that can be obtained by using a calibration technique [19].

The ESPRIT algorithm requires a subspace decomposition of the signal covariance matrix as described in [4]. The signal subspace  $\mathbf{E}_s$ , obtained from the eigendecomposition of  $\mathbf{R}_{xx}$ , is then split into two subarrays:

$$\begin{bmatrix} \mathbf{E}_x \\ \mathbf{E}_y \end{bmatrix} = \begin{bmatrix} \mathbf{J}_1 \\ \mathbf{J}_2 \end{bmatrix} \mathbf{E}_s, \quad (4.5)$$

where  $\mathbf{J}_1$  and  $\mathbf{J}_2$  are two selection matrices that depend on the subarray partition. The subarray configuration according to Fig. 4.1 yields  $\mathbf{J}_1$  and  $\mathbf{J}_2$  as follows:

$$\mathbf{J}_1 = \begin{bmatrix} 1 & 0 & 0 & 0 & 0 & 0 & 0 \\ 0 & 0 & 0 & 1 & 0 & 0 & 0 \\ 0 & 0 & 0 & 0 & 1 & 0 & 0 \\ 0 & 0 & 0 & 0 & 0 & 1 & 0 \end{bmatrix}, \quad \mathbf{J}_2 = \begin{bmatrix} 0 & 1 & 0 & 0 & 0 & 0 & 0 \\ 0 & 0 & 1 & 0 & 0 & 0 & 0 \\ 1 & 0 & 0 & 0 & 0 & 0 & 0 \\ 0 & 0 & 0 & 0 & 0 & 0 & 1 \end{bmatrix}, \quad (4.6)$$

where  $\mathbf{J}_1$  picks up elements  $\{\#0, \#3, \#4, \#5\}$  whereas  $\mathbf{J}_2$  gathers elements  $\{\#1, \#2, \#0, \#6\}$  in a subarray.

Then, the matrix  $\Psi$ , which is the solution of the ESPRIT invariance equation (4.7), is estimated using the TLS algorithm:

$$\mathbf{J}_1 \mathbf{E}_s \Psi = \mathbf{J}_2 \mathbf{E}_s \Leftrightarrow \mathbf{E}_x \Psi = \mathbf{E}_y. \quad (4.7)$$

Following the TLS algorithm, to determine the matrix  $\Psi$ , the eigendecomposition of  $\mathbf{E}_{xy}$  can be computed as follows:

$$\mathbf{E}_{xy} \stackrel{\text{def}}{=} \begin{bmatrix} \mathbf{E}_x^* \\ \mathbf{E}_y^* \end{bmatrix} \begin{bmatrix} \mathbf{E}_x & \mathbf{E}_y \end{bmatrix} \quad (4.8)$$

$$= \mathbf{E}\mathbf{\Lambda}\mathbf{E}^*, \quad (4.9)$$

where  $\mathbf{\Lambda}$  represents the diagonal matrix containing the eigenvalues of the matrix  $\mathbf{E}_{xy}$ . Then, the matrix  $\mathbf{E}$  is partitioned into four  $Q \times Q$  submatrices as follows:

$$\mathbf{E} \stackrel{\text{def}}{=} \begin{bmatrix} \mathbf{E}_{11} & \mathbf{E}_{12} \\ \mathbf{E}_{21} & \mathbf{E}_{22} \end{bmatrix}. \quad (4.10)$$

The next step consists in determining the eigenvalues  $\phi_q$  of  $\Psi = -\mathbf{E}_{12}\mathbf{E}_{22}^{-1}$ . The eigenvalue  $\phi_q$ , which is also called the phase factor, corresponds to the phase delay between the two subarrays (Fig. 4.1) for the  $q^{\text{th}}$  signal ( $q = 1, \dots, Q$ ).

Finally, the DoAs estimation  $\hat{\theta}_q$  of signals impinging the ESPAR antenna is given by:

$$\hat{\theta}_q = \sin^{-1} \left( \frac{c}{\omega_0 \Delta} \text{angle}(\phi_q) \right) + \theta_{reference}, \quad (4.11)$$

where the constant  $c$  represents the speed of propagation,  $\omega_0$  is the carrier frequency,  $\Delta$  is the norm of the vector  $\vec{\Delta}$  ( $\Delta = \lambda/4$ ),  $\text{angle}$  is a function depending on  $\phi_q$  defined by:

$$\text{angle}(\phi_q) = \tan^{-1} \left( \frac{\Im(\phi_q)}{\Re(\phi_q)} \right), \quad (4.12)$$

and  $\theta_{reference}$  is a constant angle that depends on the choice of the subarray partition.

## 4.2 Coherent Signals

Two signals  $u_1(t)$  and  $u_2(t)$  are said to be coherent if one is a scaled and delayed version of the other [9]:

$$u_1(t) = \alpha \cdot u_2(t), \quad (4.13)$$

where  $\alpha = c \cdot e^{-j \cdot a}$  is a nonrandom complex constant. The correlation coefficient  $\rho_{12}$  of these two signals defined by

$$\rho_{12} = \frac{E[u_1(t)u_2^*(t)]}{\sqrt{E[|u_1(t)|^2]E[|u_2(t)|^2]}}, \quad (4.14)$$

is equal to 1 [15], whereas  $0 \leq |\rho_{12}| < 1$  for incoherent signals.

However, we assume that the signals  $u_1$  and  $u_2$  can be qualified as coherent if they are highly correlated ( $|\rho_{12}| > 0.9$ ).

In our simulations, the correlation coefficient  $\rho_{12}$  between signals  $u_1[k]$  and  $u_2[k]$  is estimated as follows:

$$\hat{\rho}_{12} = \frac{\sum_{k=1}^K u_1[k]u_2^*[k]}{\sqrt{\sum_{k=1}^K |u_1[k]|^2 \sum_{k=1}^K |u_2[k]|^2}}, \quad (4.15)$$

where  $K$  represents the number of symbols defining signals  $u_1[k]$  and  $u_2[k]$ . This means that in the simulations, we heuristically built two signals  $u_1$  and  $u_2$  with a desired value of  $\hat{\rho}_{12}$ .

Generally, coherent signals appears in an indoor multipath propagation environment. Indeed, in wireless communications environment, mutipath propagation implies that the original signal and the reflected signal are coherent.

### 4.3 Simulation Results with Two Highly Correlated Signals

Simulations were performed with two highly correlated signals to evaluate the influences of three main parameters on the DoA estimation performance while employing the ESPRIT algorithm for ESPAR antenna. These three main parameters, which characterize the propagation environment, in our simulations, are the signal to noise ratio (SNR), the correlation coefficient  $\rho$ , and the angular distance  $\Delta\theta$  between the two signals.

#### 4.3.1 Simulation protocol

Simulations were performed with the following conditions:

- The number of signals impinging the ESPAR antenna is assumed to be known and is equal to 2.
- $K = 10\,000$  samples define the number of signal samples (see Fig. 4.2).
- $N = 2\,000$  independent trial runs were conducted; for each trial run, noise and signal samples are redefined.
- The SNR is fixed to 25 dB, except in Fig. 4.3.

- The two signals impinging the ESPAR antenna arrive from DoAs  $\theta_1 = 35^\circ$  and  $\theta_2 = 145^\circ$ , except in Fig. 4.6, and
- The average estimation error  $\varepsilon$  is computed as an average of the estimation errors of the trial runs:

$$\varepsilon = \frac{1}{N} \sum_{n=1}^N |\hat{\theta}_n - \theta|, \quad (4.16)$$

where  $\hat{\theta}_n$  corresponds to the DoA estimation associated to the  $n^{\text{th}}$  trial and  $\theta$  represents the signal DoA.

### 4.3.2 Influence of the correlation coefficient $\rho$ and SNR value on the DoA estimation performance

This section examines the effect of SNR value and correlation coefficient  $\rho$  on the resulting DoA estimation.

The first simulation (Fig. 4.3) evaluates the effect of these two parameters, and simulations have been carried out for correlation coefficient values of 0, 0.9, 0.95 and 0.99, with the SNR value increasing from 0 dB to 35 dB.  $\rho = 0$  represents the performance of the ESPRIT algorithm for ESPAR antenna in the case of uncorrelated signals, as studied in [4]. We can notice that

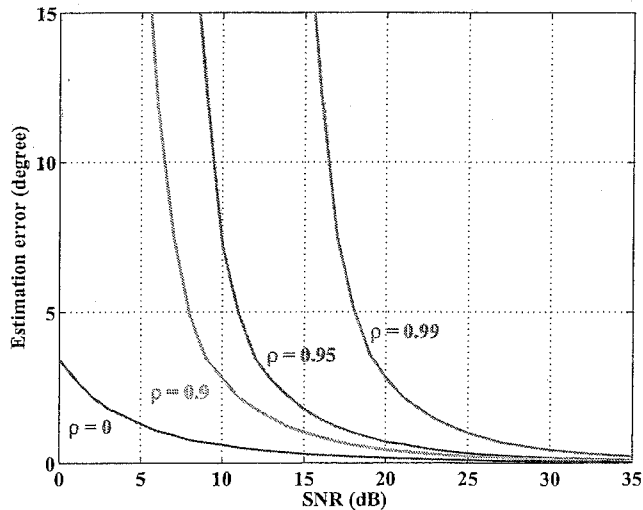


FIGURE 4.3: Influence of SNR on DoA estimation performance for two uncorrelated and highly correlated signals. The DoAs are  $\theta_1 = 35^\circ$ ;  $\theta_2 = 145^\circ$ .

the higher the correlation coefficient  $\rho$  is, the more important the effect of the SNR is. Indeed, the curves corresponding to the uncorrelated case ( $\rho = 0$ ) and the highly correlated case ( $\rho = 0.99$ ) clearly illustrate the influence of the correlation coefficient  $\rho$  on the DoA estimation performance of the ESPRIT algorithm for ESPAR antenna. Observing the curve corresponding to  $\rho = 0.99$ , we can state that for an SNR higher than 20 dB, the estimation error is smaller than 3 degrees, rather than for a  $\rho = 0.95$ , the estimation error is smaller than 3 degrees for an SNR higher than 12.5 dB.

The second simulation (Fig. 4.4) evaluated the sensitivity of the ESPRIT algorithm for ESPAR antenna to the correlation coefficient  $\rho$ . The SNR was fixed to 25 dB. The correlation coefficient  $\rho$  of the two signals increases from 0.95 to a value close to 1. Fig. 4.4 shows that the accuracy of the DoA es-

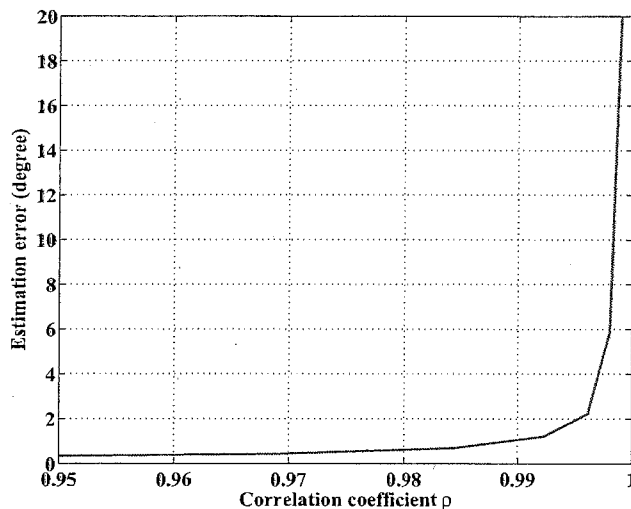


FIGURE 4.4: Influence of the correlation coefficient on DoA estimation performance. DoAs are  $\theta_1 = 35^\circ$ ,  $\theta_2 = 145^\circ$ ,  $SNR = 25$  dB, 2 000 trial runs.

timation relies on the value of the coefficient correlation  $\rho$ , in particular for  $\rho > 0.9$ . Indeed, Fig. 4.4 shows that the estimation error increases in an exponential way. The error estimation  $\varepsilon$  quickly grows from  $\rho = 0.995$ .

Therefore, the DoA estimation performance decreases as the correlation coefficient increases.

### 4.3.3 Angular variation influence on DoA estimation

In this section, the resolution threshold for two arrival signals with an angular difference of  $\Delta\theta$  is investigated (Fig. 4.6). The angular difference  $\Delta\theta$  between DoAs  $\theta_1$  and  $\theta_2$  ( $\Delta\theta = |\theta_2 - \theta_1|$ ) increases in steps of  $2^\circ$  from  $0^\circ$  to  $180^\circ$  as shown in Fig. 4.5. Thus,  $\theta_1$  varies from  $90^\circ$  to  $0^\circ$ , whereas  $\theta_2$  increases from  $90^\circ$  to  $180^\circ$ . We can observe that for  $\Delta\theta$  between  $40^\circ$  and  $160^\circ$ ,

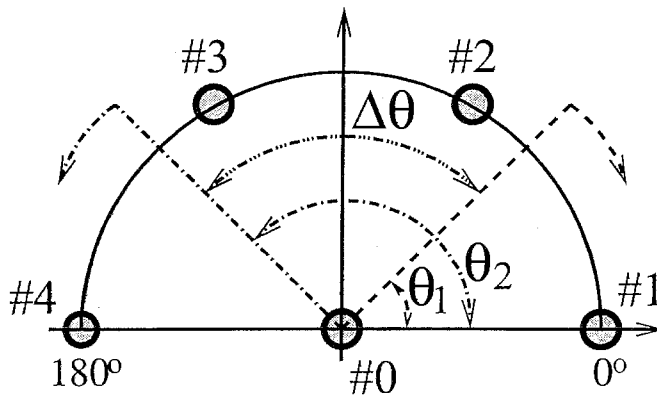


FIGURE 4.5: Variation in angular difference between signals.

the ESPRIT algorithm for ESPAR antenna can correctly estimate DoAs of highly correlated signals. However, below an angular difference of  $40^\circ$ , the estimation degrades. This degradation of DoA estimation is due to the fact that the signals are too close together. Another observable behavior is the increasing estimation error after  $\Delta\theta = 160^\circ$ , which is due to a side effect on the antenna endfire, as explained in [4].

On the other hand, we can observe that the performance of the ESPRIT algorithm for ESPAR antenna decreases as the correlation coefficient  $\rho$  increases. Indeed, for a correlation coefficient 1.04 times higher than 0.95 (0.99), the averaged estimation error is 5.5 times higher for an angular difference  $\Delta\theta = 40^\circ$ .

Finally, we can notice that the minimal error is reached for an angular difference equal to  $120^\circ$ , which corresponds to signals, DoAs at  $\theta_1 = 30^\circ$  and  $\theta_2 = 150^\circ$ .



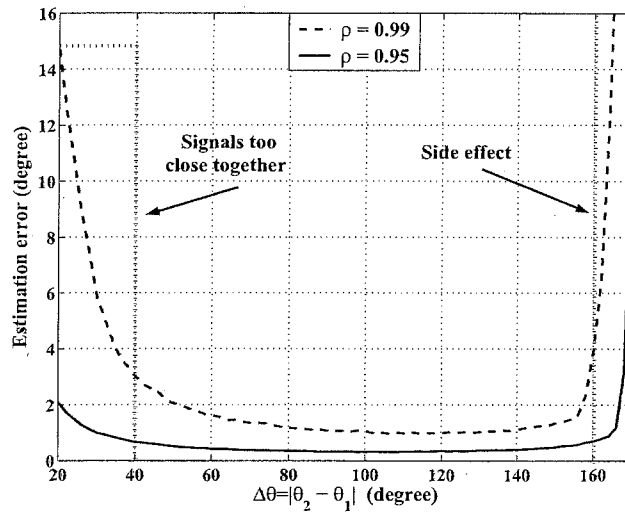


FIGURE 4.6: Influence of angular variation in DoA estimation error ( $\varepsilon$ ) for coherent signals, with an angular distance of  $\Delta\theta$  between the two signals;  $\rho$  denotes the correlation coefficient between the two signals, SNR=25 dB.



## Chapter 5

# The ESPRIT Algorithm for ESPAR Antennas Combined with Forward-Backward Averaging Technique

### 5.1 Forward-Backward Averaging Technique Combined with the ESPRIT Algorithm for ESPAR Antenna

Different documents and articles relate to the forward-backward averaging technique [1, 2, 7, 16]. A previous adaptation of the FBA technique has been presented for the reactance domain MUSIC algorithm for ESPAR antenna, which also uses spatial smoothing processing [7]. However, in the case of the ESPRIT algorithm for ESPAR antenna, due to the invariance requirement, a specific adaptation of [7] was needed.

The principle of the FBA technique applied with the ESPRIT algorithm (FBA-ESPRIT algorithm) for ESPAR antenna is to modify the covariance matrix  $\mathbf{R}_{xx}$  computed in (4.4) to obtain the properties of an equivalent linear antenna. Employing a transform matrix  $\mathbf{T}$ , the elements of  $\mathbf{R}_{xx}$  are arranged as shown in Fig. 5.1. This modification is computed as follows:

$$\mathbf{R}_{xx}^{(r1)} = \mathbf{T}\mathbf{R}_{xx}\mathbf{T}^T, \quad (5.1)$$

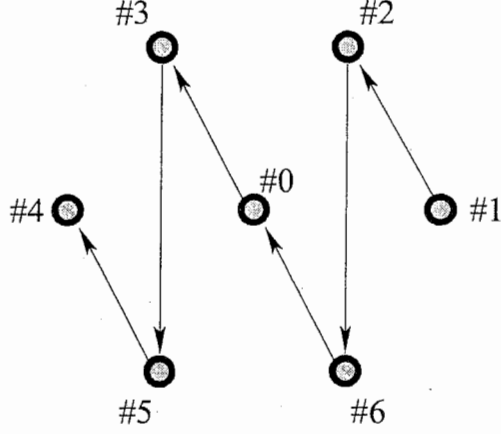


FIGURE 5.1: Reordering of the elements of the antennas.

where

$$\mathbf{T} = \begin{bmatrix} 0 & 1 & 0 & 0 & 0 & 0 & 0 \\ 0 & 0 & 1 & 0 & 0 & 0 & 0 \\ 0 & 0 & 0 & 0 & 0 & 0 & 1 \\ 1 & 0 & 0 & 0 & 0 & 0 & 0 \\ 0 & 0 & 0 & 1 & 0 & 0 & 0 \\ 0 & 0 & 0 & 0 & 0 & 1 & 0 \\ 0 & 0 & 0 & 0 & 1 & 0 & 0 \end{bmatrix}. \quad (5.2)$$

Next, the correlation matrix  $\mathbf{R}_{\mathbf{xx}}^{(FBA)}$  is computed by applying the forward-backward averaging technique to  $\mathbf{R}_{\mathbf{xx}}^{(\tau 1)}$ :

$$\mathbf{R}_{\mathbf{xx}}^{(FBA)} = \frac{1}{2}(\mathbf{R}_{\mathbf{xx}}^{(\tau 1)} + \mathbf{J}\mathbf{R}_{\mathbf{xx}}^{(\tau 1)*}\mathbf{J}), \quad (5.3)$$

where  $\mathbf{J}$  is an  $(M + 1) \times (M + 1)$  exchange matrix with ones on the anti-diagonal and zeros elsewhere:

$$\mathbf{J} = \begin{bmatrix} 0 & \dots & 0 & 1 \\ 0 & \dots & 1 & 0 \\ \vdots & \diagup & \vdots & \vdots \\ 1 & \dots & 0 & 0 \end{bmatrix}. \quad (5.4)$$

Then,  $\mathbf{R}_{\mathbf{xx}}^{(FBA)}$  must be arranged in order to maintain the translational invariance property of the regular hexagonal shaped ESPAR antenna (Fig. 4.1).

$$\mathbf{R}_{\mathbf{xx}}^{(\tau 2)} = \mathbf{T}^T \mathbf{R}_{\mathbf{xx}}^{(FBA)} \mathbf{T}. \quad (5.5)$$

Indeed, elements of  $\mathbf{R}_{xx}^{(FBA)}$  must be in the same order as  $\mathbf{R}_{xx}^{(r1)}$  to apply the ESPRIT algorithm for ESPAR antenna with selection matrices  $\mathbf{J}_1$  and  $\mathbf{J}_2$ . Finally, we can apply the ESPRIT algorithm for ESPAR antenna to the matrix  $\mathbf{R}_{xx}^{(r2)}$  instead of  $\mathbf{R}_{xx}$ , as explain in Sec. 4.1.

## 5.2 Simulation Results of DoA Estimation Employing FBA-ESPRIT Algorithm for ESPAR Antenna

In this section, some simulations of DoA estimation illustrate the performance of the FBA-ESPRIT algorithm for ESPAR antenna compared to the standard ESPRIT algorithm for ESPAR antenna. Simulations were performed with two coherent signals.  $K = 10\,000$  snapshots defined the number of snapshots per signal (see Fig. 4.2), thus a total of  $(M + 1) \times K$  snapshots are used to compute  $\hat{\mathbf{R}}_{yy}$ . For each simulation,  $N = 2\,000$  independent trial runs are used to evaluate the performance of the FBA-ESPRIT algorithm for ESPAR antenna (see Sec. 4.3.1).

The first simulation (Fig. 5.2) clearly showed the robustness of the FBA-ESPRIT algorithm for ESPAR antenna. Indeed, in a noise-free environment, the forward-backward averaging technique can perfectly resolve highly correlated signals. Figure 5.2 shows that the estimation error exponentially increases with the ESPRIT algorithm for ESPAR antenna whereas the FBA technique makes it possible to decorrelate coherent signals.

The second simulation was conducted to evaluate the DoA estimation in a noisy environment. This simulation was performed under similar conditions for the ESPRIT algorithm for ESPAR antenna and the FBA-ESPRIT algorithm for ESPAR antenna. Figure 5.3 shows that, in a noisy and coherent environment, the performance of the forward-backward technique is slightly better than that of the standard ESPRIT algorithm for ESPAR antenna. Therefore, the forward-backward technique does not deteriorate the DoA estimation of the original ESPRIT algorithm for ESPAR antenna.

In a low noisy environment and in the case of coherent signals, the FBA technique allows us to improve the DoA estimation performance. Indeed, Fig. 5.4 shows a DoA estimation error improvement of about  $5^\circ$ . When  $\Delta\theta$  is between  $40^\circ$  and  $140^\circ$ , the DoA estimation improves by about 29% to 64%. Furthermore, Fig. 5.4 shows an estimation degradation when  $\Delta\theta < 40^\circ$  on account of the signals being too close together. Moreover, in the case where  $\Delta\theta > 140^\circ$ , the degradation is due to a side effect, as explained in [4] and Fig. 4.6.

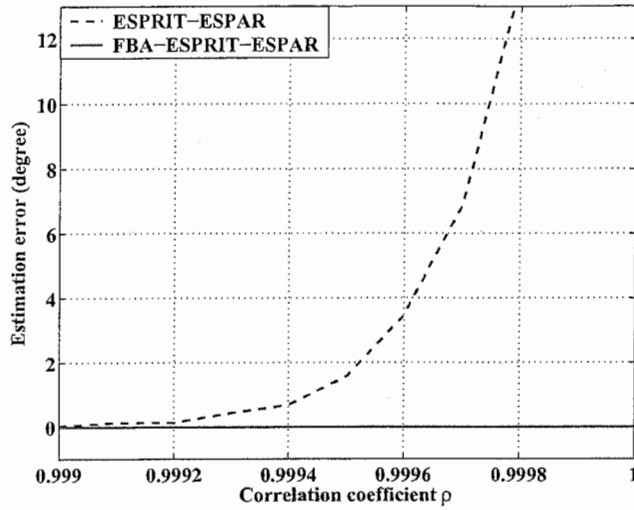


FIGURE 5.2: Effect of FBA on decorrelation of two coherent signals in a noise-free environment ( $SNR = \infty$ ). The DoAs are  $\theta_1 = 35^\circ$ ,  $\theta_2 = 145^\circ$ ; 2000 independent trial runs.

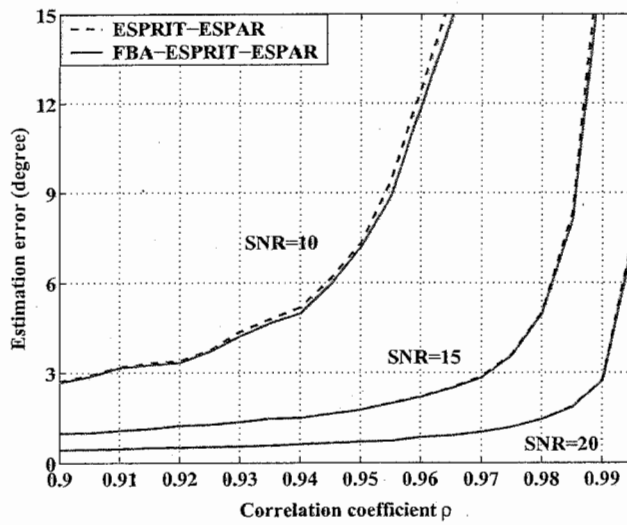


FIGURE 5.3: Effect of SNR on DoA estimation. The DoAs are  $\theta_1 = 35^\circ$ ,  $\theta_2 = 145^\circ$ ; 2000 independent trial runs.

The final simulation showed that the forward-backward averaging technique allows us to propose a simple reliability criterion for the DoA estima-

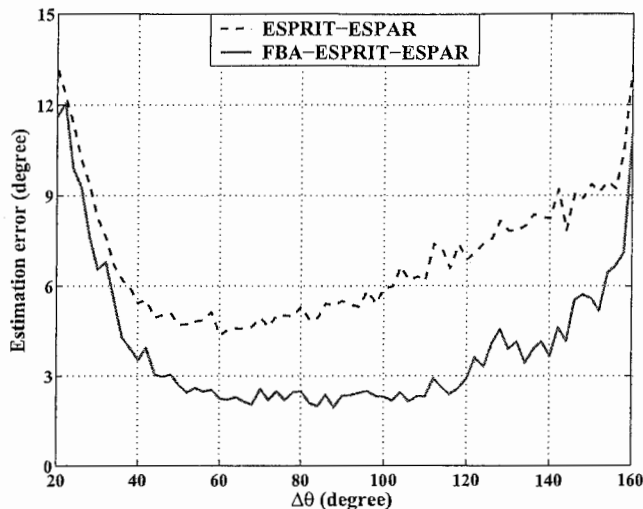


FIGURE 5.4: Effect of FBA on ESPRIT for ESPAR for two coherent signals with angular distance  $\Delta\theta = |\theta_2 - \theta_1|$  (SNR=40 dB; correlation coefficient  $\rho = 0.9997$ , 2 000 independent trial runs).

tion [6]. Indeed, the simulation shows that the phase factors will be constraint on the unit-circle. So, analogously to the conventional ESPRIT algorithm for ESPAR antenna, we state a criterion on the reliability of the estimates. When the FBA-ESPRIT algorithm for ESPAR antenna successfully estimates the signal DoA, the phase factors  $\phi_q$  ( $q = 1, \dots, Q$ ) should be constrained on the unit-circle. Therefore, we can state a criterion on the reliability of the estimates. When the FBA-ESPRIT algorithm for ESPAR antenna successfully estimates the signal DoA, the phase factors are constrained on the unit-circle.

Figure 5.5 shows results of simulations in coherent situations for the ESPRIT algorithm for ESPAR antenna and the FBA-ESPRIT algorithm for ESPAR antenna. This simulation clearly shows that, using the forward-backward averaging technique, the phase factors of the estimations are precisely on the unit-circle in the complex plane. This reliability criterion is based on the fact that the eigenvalues  $\phi_q$  of  $\Psi$  (4.7) have to satisfy the following relation:

$$|\phi_q| = 1. \quad (5.6)$$

If the relation  $|\phi_q| = 1$  is satisfied, the phase factor  $\phi_q$  is on the unit-circle and the corresponding estimates  $\hat{\theta}_q$  is said to be reliable. In the contrary, the corresponding estimates is said to be unreliable and can be discarded.

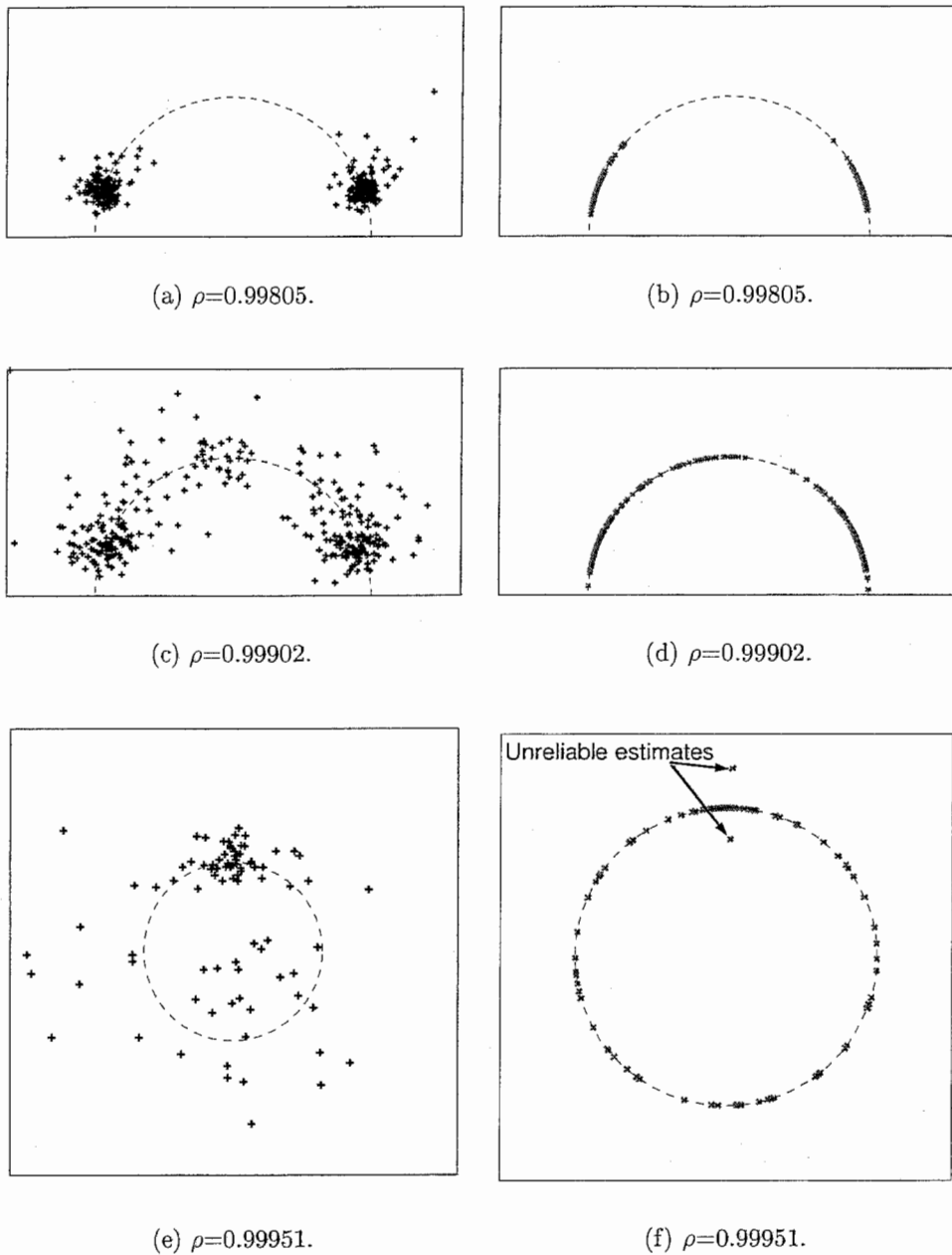


FIGURE 5.5: Scatter of phase factors  $\phi_1$  and  $\phi_2$  for two coherent signals with correlation coefficient  $\rho$ , employing ESPRIT for ESPAR(5.5(a), 5.5(c) and 5.5(e)) and FBA-ESPRIT for ESPAR(5.5(b), 5.5(d) and 5.5(f)). SNR=25 dB, 300 trial runs (except for: 5.5(e) and 5.5(f): 50 trial runs).



## CONCLUSION

In this report, the ESPRIT algorithm for ESPAR antenna was applied to coherent signals for the first time. This algorithm could estimate DoAs of correlated signals. However, in the case of coherent signals (*i.e.*, highly correlated signals), degradation of performance was observed.

To improve the DoA estimation performance in the case of coherent signals, the forward-backward averaging technique was combined with the standard ESPRIT algorithm for ESPAR antenna. Simulations show that the forward-backward averaging technique can perfectly resolve coherent signals in the noise-free case. In a noisy and highly correlated environment, this technique is still valid since the FBA technique does not deteriorate the DoA estimation performance of the ESPRIT algorithm for ESPAR antenna. Furthermore, FBA-ESPRIT for ESPAR provides a reliability criterion for the DoA estimates. This criterion represents a new way to indicate whether estimates are reliable or not. Moreover, by employing the FBA technique, the computational complexity of the algorithm does not increase. Accordingly, the FBA-ESPRIT algorithm for ESPAR antenna represents an improved version of the standard ESPRIT algorithm for ESPAR antenna. Therefore our proposed method can be used in place of the standard ESPRIT algorithm for ESPAR antenna.





## ACKNOWLEDGEMENTS

I would like to express my gratitude to Mr. Eddy Taillefer and Mr. Tomoyuki Aono, who were excellent supervisors and who introduced me to the Wave Engineering Laboratories. I also thank Dr. Takashi Ohira, head of Department of Radio Waves, and Dr. Bokuji Komiyama, president of the Wave Engineering Laboratories, for their helpful encouragements and their interests to my work.

I would like to take the opportunity to thank the entire WEL Department of Radio Waves members, Mr. Victor Briend, Dr. Qing Han, Mr. Keisuke Higuchi, Mr. Akifumi Hirata, Dr. Thomas Hunziker, Mr. Kyouchi Igusa, Mr. Mathieu Lenoble, Mr. Takuma Sawaya, Mr. Tatsuya Shimizu, Dr. Chen Sun, Dr. Makoto Taromaru and Mr. Makoto Yamamoto for their collaboration and discussion.

I would like to express my gratitude to Ms. Naoko Nakaya and the SHIEN group for their help in filling the numerous formality papers and the procedures to come in Japan.

Finally, I would like to thank all the ATR staff for their friendship and kindness.



# Bibliography

- [1] Rainer Bachl. The forward-backward averaging technique applied to TLS-ESPRIT processing. In *IEEE Transactions on Signal Processing*, volume 43, pages 2691–2699, November 1995.
- [2] B. Chandna and Amit Mahadar. 2D beamspace ESPRIT with spatial smoothing. In *IEEE Antennas and Propagation Society International Symposium*, volume 1, pages 219–222, 21–26 June 1998.
- [3] Sathish Chandran, editor. *Adaptive Antenna Arrays: Trends and Applications*, chapter Analog Smart Antennas. Springer-Verlag, 2004. ISBN 3-540-20199-8.
- [4] Emmanuelle Chu, Eddy Taillefer, and Takashi Ohira. Direction-of-arrival estimation with a seven-element regular-hexagonal shaped ESPAR antenna employing ESPRIT algorithm. In *IEICE Antenna and Propagation Technical Meeting*, pages 19–24, Sendai, August 2003.
- [5] Koichi Gyoda, Yuichiro Ohno, Youito Kado, and Takashi Ohira. Wacnet: Wireless ad-hoc community network. In *IEEE International Conference on Industrial Electronics, Control and Instrumentation*, pages 1153–1158, Nagoya Japan, October 22<sup>nd</sup>-28<sup>th</sup> 2000.
- [6] Martin Haardt and Josef A. Nosske. Unitary ESPRIT: How to obtain increased estimation accuracy with a reduced computational burden. In *IEEE Transactions on Signal Processing*, volume 43, pages 1232–1242, May 1995.
- [7] Akifumi Hirata, Tomoyuki Aono, Hiroyoshi Yamada, and Takashi Ohira. Reactance-domain SSP MUSIC for an ESPAR antenna to estimate the DoAs of coherent waves. In *The 6th International Symposium on Wireless Personal Multimedia Communications (WPMC'03)*, pages 242–246, 2003.

- [8] Akifumi Hirata, Jun Cheng, Masaya Hashiguchi, and Takashi Ohira. Reactance-domain signal processing for ESPAR antennas - spatial correlation and correlation matrix -. *IEICE Technical report RCS2002-148*, 102(282):9–14, Aug. 2002. in Japanese.
- [9] Hamid Krim and Mats Viberg. Two decades of array signal processing research: The parametric approach. *IEEE Signal Processing Magazine*, 13(4):67–94, July 1996.
- [10] Mathieu Lenoble, Thomas Hunziker, and Takashi Ohira. Direction-of-arrival and time-delay estimation with an ESPAR antenna employing SAGE algorithm. In *IEICE Antenna and Propagation Technical Meeting*, Sendai, August 2003.
- [11] Yoshihiko Ogawa, Akifumi Hirata, Hiroyoshi Yamada, and Takashi Ohira. Experiment of DoA estimation with RD-CUBA-MUSIC using 7-element ESPAR antennas. In *Proceedings of ISAP'04*, pages 1309–1312, 2004.
- [12] Takashi Ohira and Koichi Gyoda. Hand-held microwave direction-of-arrival finder based on varactor-tuned analog aerial beamforming. In *IEEE Asia-Pacific Microwave Conference*, volume 2, pages 585–588, Taipei, Taiwan, Dec. 2001.
- [13] Mickaël Pencolé, Eddy Taillefer, Tomoyuki Aono, and Takashi Ohira. Direction-of-arrival estimation of two coherent signals employing the ESPRIT algorithm for ESPAR antenna. In *IEICE, Radio Communication Systems*, Niigata, October 2004.
- [14] Mickaël Pencolé, Eddy Taillefer, Tomoyuki Aono, and Takashi Ohira. Forward-backward averaging technique applied to ESPRIT algorithm for a 7-element ESPAR antenna. In *IEICE, General Conference*, volume B-1-170, page 170, Tokushima, September 2004.
- [15] S. Unnikrishna Pillai. *Array Signal Processing*. Springer-Verlag, 1989.
- [16] S. Unnikrishna Pillai and Byung Ho Kwon. Forward/backward spatial smoothing techniques for coherent signal identification. *IEEE Transactions on Acoustics, Speech, and Signal Processing*, 37:8–15, Jan. 1989.
- [17] Cyril Plapous, Jun Cheng, Eddy Taillefer, Akifumi Hirata, and Takashi Ohira. Reactance domain MUSIC algorithm for electronically steerable parasitic array radiator antenna. *IEEE Transactions on Antennas and Propagation*, Feb. 2005.

- [18] Richard Roy and Thomas Kailath. ESPRIT- estimation of signal parameters via rotational invariance techniques. In *IEEE Transactions on Acoustics, Speech, and Signal Processing*, volume 37, pages 984–995, July 1989.
- [19] C.M.S. See. Sensor array calibration in presence of mutual coupling and unknown sensor gains and phases. In *Electronics Letters*, volume 30, pages 373–374, March 3<sup>rd</sup> 1994.
- [20] Blagovest Shishkov, Jun Cheng, and Takashi Ohira. Adaptive control algorithm of ESPAR antenna based on stochastic approximation theory. *IEICE Trans. Comm.*, E85-B(4):802–811, April 2002.
- [21] A. Lee Swindlehurst, Björn Ottersten, Richard Roy, and Thomas Kailath. Multiple invariance esprit. In *IEEE Transactions on Signal Processing*, volume 40, pages 867–881, April 1992.
- [22] Eddy Taillefer, Akifumi Hirata, and Takashi Ohira. Direction-of-arrival estimation using radiation power pattern with an ESPAR antenna. *IEEE Transactions on Antennas and Propagation*. accepted for publication.
- [23] Mati Wax and Thomas Kailath. Detection of signals by information theoretic criteria. In *IEEE Transactions on Acoustics, Speech, and Signal Processing*, volume ASSP-33, pages 387–392, April 1985.





# APPENDIX A : MATLAB SOURCE CODES

## creer\_2sigcorr.m

<pre>program name: creer_2sigcorr.m comments: Generate 2 correlated signals</pre>
---

```
function [symb, erho, ecov] = creer_2sigcorr (P, rho)
%
% [symb,rrho] = creer_2sigcorr (P, rho)
%
% Cree 2 signaux ayant un coefficient de correlation voulu: rho
%
% P      : nombre de symboles
% rho    : coefficient de correlation voulu
% symb   : les symboles
% erho   : le coefficient de correlation pour les symboles generes
% ecov   : cov(X,Y) = cor(X,Y) - E[X]*E[Y]
%
% -- P grand tu choisiras du rho voulue tu seras proche --

% D'abord on cree deux vecteurs parfaitement non correles
nsymb = 1-2*randint(1,P,2);

symb = zeros(2,P);
symb(1,1:2:P) = nsymb(1:2:P);
symb(1,2:2:P) = nsymb(2:2:P);
symb(2,1:2:P) = nsymb(1:2:P);
symb(2,2:2:P) = -nsymb(2:2:P);

% Puis on les melange aleatoirement sur une longueur de rho*P
```

```

nb = floor(P*rho);

% version rapide avec randperm
selsym = zeros(1,nb);

vals = randperm(P);
indice = randint(1,1,[1 P-nb]); % distribution uniforme centree
selsym = vals(indice:indice+nb-1);

%% version simple mais non optimisee (tres lent si P grand)
% for indice=1:nb
%     val = randint(1,1,[1 P]);
%     while (length(find(selsym==val))~=0)
%         val = randint(1,1,[1 P]);
%     end
%     selsym(indice) = val;
% end
symb(1,selsym) = symb(2,selsym);

%symb(3,:) = symb(1,:);

C = symb*symb'/P;
erho = C(1,2);
ecov = erho - mean(symb(1,:))*mean(symb(2,:));

```

## esprit\_sans\_fb.m

<p><b>program name:</b> esprit_sans_fb.m <b>comments:</b> ESPRIT algorithm for ESPAR antenna without FBA technique</p>
--

```
function [doae, doa, ags, phi] = esprit_sans_fb(x, P, M, J1, J2, pa, W, K,
J, doas)

%
% [doae, doa, ags, phi] = esprit_sans_fb(x, P, M, J1, J2, pa, W, K, J, doas)
%
% ESPRIT algorithm for ESPAR antenna without FBA technique
%

rad2deg = 180/pi;          % radian to degree
deg2rad = pi/180;         % degree to radian

% reactance-domain correlation matrix Ryy
Ryy = x*x'/P;
[Uy,Sy,Vy]=svd(Ryy);      % singular value decomposition of Ryy

% Estimation of the noise covariance matrix Rnn=sigma*eye(M)
sigma = sum(diag(Sy(pa+1:M,pa+1:M)))/(M-pa);

% Element-space correlation matrix Rxx
Rxx = inv(W)*(Ryy-sigma*eye(M))*inv(W');

% Eigendecomposition of Rxx to obtain the signal subspace Es
[Uxx, Sxx, Vxx] = svd(Rxx);
Es = Uxx(:,1:pa);

% Decomposition of Es
Ux =J1*Es;
Uy =J2*Es;

% Eigenvalues of the matrix Phi, which is solution of the ESPRIT invariance
% equation
Uz = [Ux'*Ux Ux'*Uy; Uy'*Ux Uy'*Uy];
[U,S,V]=svd(Uz);
Vn= V(:,pa+1:2*pa);
Phi = -Vn(1:pa,:)*inv(Vn(pa+1:2*pa,:));
[Up,Sp,Vp] = svd(Phi);
```

```
phi = eig(Phi);

% Direction of Arrival estimation
doae = asin((2/pi)*atan(imag(phi)./real(phi)))*rad2deg + 90 ;
doa = phi*exp(sqrt(-1)*pi/2);
ags = exp(sqrt(-1)*doas*deg2rad);
```

## esprit\_avec\_fb.m

<pre>program name: esprit_avec_fb.m comments: ESPRIT algorithm for ESPAR antenna with FBA technique</pre>
---

```
function [doae, doa, ags, phi] = esprit_avec_fb(x, P, M, J1, J2, pa, W, K,
J, doas)

%
% [doae, doa, ags, phi] = esprit_avec_fb(x, P, M, J1, J2, pa, W, K, J, doas)
%
% ESPRIT algorithm for ESPAR antenna combined with FBA technique
%

rad2deg = 180/pi;      % radian to degree
deg2rad = pi/180;     % degree to radian

% reactance-domain correlation matrix Ryy
Ryy = x*x'/P;
[Uy,Sy,Vy]=svd(Ryy);  % singular value decomposition of Ryy

% Estimation of the noise covariance matrix Rnn=sigma*eye(M)
sigma = sum(diag(Sy(pa+1:M,pa+1:M)))/(M-pa);

% Element-space correlation matrix Rx
Rx = inv(W)*(Ryy-sigma*eye(M))*inv(W');

% Transform matrix T
tmp = diag(ones(1,M));
T = tmp([2 3 7 1 4 6 5],:);

% Change the order of the element of Rx, and FBA technique
Rxx = T.'*((T*Rx*T.'+J*conj(T*Rx*T.')*J)/2)*T;

% ESPRIT algorithm for ESPAR antenna applied to Rxx
[Uxx, Sxx, Vxx] = svd(Rxx);
Es = Uxx(:,1:pa);
En = Uxx(:,pa+1:M);
Ux = J1*Es;
Uy = J2*Es;
Uz = [Ux'*Ux Ux'*Uy; Uy'*Ux Uy'*Uy];
[U,S,V]=svd(Uz);
```

```

Vn= V(:,pa+1:2*pa);
Phi = -Vn(1:pa,:)*inv(Vn(pa+1:2*pa,:));
[Up,Sp,Vp] = svd(Phi);
phi = eig(Phi);

% Direction of Arrival estimation
doae = asin((2/pi)*atan(imag(phi)./real(phi)))*rad2deg + 90 ;
doa = phi*exp(sqrt(-1)*pi/2);
ags = exp(sqrt(-1)*doas*deg2rad);

```

## cal\_w.m

```
program name: cal_w.m
comments: Generate the weight matrix W
```

```
function [W] = cal_w(react,M)

y00 = 0.00023344-j*0.0066918;
y10 = -0.0001816+j*0.00242469;
y11 = 0.00300676-j*0.0044176;
y21 = 0.00097427+j*0.00299986;
y31 = -0.0003066-j*0.0003067;
y41 = 0.0000973-j*0.0001353;

Y = [y00 y10 y10 y10 y10 y10 y10;
     y10 y11 y21 y31 y41 y31 y21;
     y10 y21 y11 y21 y31 y41 y31;
     y10 y31 y21 y11 y21 y31 y41;
     y10 y41 y31 y21 y11 y21 y31;
     y10 y31 y41 y31 y21 y11 y21;
     y10 y21 y31 y41 y31 y21 y11];

Z = inv(Y);
u0 = [1 0 0 0 0 0 0].';

zs = 50;

% Calculate the weight matrix W
W = zeros(M,M);
for index= 1:M
    W(index,:) = (2*zs*inv(Z+diag([zs;j*react(index,:).']))*u0).';
end
```





# APPENDIX B : INFLUENCE OF CORRELATION COEFFICIENT $\rho$ , SNR AND ANGULAR DISTANCE BETWEEN SIGNALS ON DOA ESTIMATION

esprit\_var\_rho.m

<pre>program name: esprit_var_rho.m comments: Investigation of the influence of the angular distance between signals</pre>
--

```
%
% Teste l'influence de la valeur du coefficient de corrélation
% rho sur la performance d'estimation des DoAs en employant
% ESPRIT pour ESPAR et FBA-ESPRIT pour ESPAR
%
clear all;
clf;
close all;

tps = clock;                % horloge au debut de la simulation

P = 10000;                  % Number of snapshot to define a signal
SNR = 22;                   % Signal to Noise Ratio (dB)
doas = [35 145];           % DoAs of signals
NB_ITERATIONS = 50;        % Number of trials
rho = 0;                    % correlation coefficient of the two signals
```

```

pas_incrementation = 0.05; % pas pour incrementer la valeur de rho
alpha1 = 0.000000000001; % Couronne de validite autour du cercle unite
                                % pour le critere de validite
M =7;                            % Number of elements of the ESPAR antenna
x0 = 50;

rad2deg = 180/pi;
deg2rad = pi/180;

e11 = [1 0 0 0].';
e12 = [0 1 0 0].';
e13 = [0 0 1 0].';
e14 = [0 0 0 1].';
zer = [0 0 0 0].';

J = fliplr(diag(ones(1,M)));

react = [ 0 0 0 0 0 0 ;
          300 300 -300 -300 -300 300;
          300 300 300 -300 -300 -300;
          -300 300 300 300 -300 -300;
          -300 -300 300 300 300 -300;
          -300 -300 -300 300 300 300;
          300 -300 -300 -300 300 300
        ];

W = cal_w(react,M);

nb_mesures = 0;                % initialisation du nombre de mesures
                                % (1 mesure = 1 valeur de rho particuliere)

while (rho <= 0.9999)
    nb_mesures = nb_mesures + 1
    mean_angle = 0;            % valeur moyenne des angles estimes avec la 1ere
                                % methode (FBA-ESPRIT-ESPAR)
    mean_angle2 = 0;          % valeur moyenne des angles estimes avec la
                                % 2eme methode (ESPRIT-ESPAR)
    sum_angle(1:2) = 0;        % Somme des angles estimes avec la 1ere methode
    sum_angle2(1:2) = 0;      % Somme des angles estimes avec la 2eme methode
    sum_erreur(1:2) = 0;
    sum_erreur2(1:2) = 0;
    nb_estimations = 0;       % nombre de signaux estimes avec la 1ere methode
    nb_estimations2 = 0;      % nombre de signaux estimes avec la 2eme methode

```

```

clear resultat_constellation;
clear resultat_constellation2;
clear probaX;
clear probaX2;
for indice_iteration = 1 : NB_ITERATIONS

    J1 = [el3, el1, el2, zer, zer, zer, el4]; % Matrice de selection J1
    J2 = [el1, zer, zer, el2, el3, el4, zer]; % Matrice de selection J2
    K = [J1;J2];
    [symbols, erho, ecov] = creer_2sigcorr(P, rho);
    nsig = length(doas);
    noise = randn(7,P) + sqrt(-1)*randn(7,P);

    [nsig,P] = size(symbols);

    % 1ere Methode : Forward-Backward combine avec ESPRIT-ESPAR
    % -----
    A = [
            ones(1,nsig);
        exp(sqrt(-1)*(pi/2)*cos(deg2rad*doas));
        exp(sqrt(-1)*(pi/2)*cos(deg2rad*(doas-60)));
        exp(sqrt(-1)*(pi/2)*cos(deg2rad*(doas-120)));
        exp(sqrt(-1)*(pi/2)*cos(deg2rad*(doas-180)));
        exp(sqrt(-1)*(pi/2)*cos(deg2rad*(doas-240)));
        exp(sqrt(-1)*(pi/2)*cos(deg2rad*(doas-300)))
    ];

    psym = diag((symbols*symbols')/P);

    % Tous les signaux ont le meme SNR
    sig = diag(sqrt((2*(10.^(SNR/10.0)))./psym)) * symbols;
    x = ((W*A)*sig) + noise;
    pa=nsig;
    [doae, doa, ags, phi, Rxx, Rxx1, Phi] = esprit_avec_fb(x, P, M, J1,
        J2, pa, W, K, J, doas);
    if length(find((1-alpha1)<=abs(phi) & abs(phi)<=(1+alpha1))) == nsig
        sum_angle = sum_angle + sort(doa.'');
        sum_erreur = sum_erreur + abs(sort(doa.'')-sort(doas));
        nb_estimations = nb_estimations + 1;
        tab_estimation(nb_estimations,:) = [doae.' doa.' ags];
        % enregistrement des resultats
        resultat_constellation(nb_estimations,1) = rho;
        resultat_constellation(nb_estimations,2) = erho;
        resultat_constellation(nb_estimations,3:4) = doae.';
    end
end

```

```

resultat_constellation(nb_estimations,5:6) = doa.';
resultat_constellation(nb_estimations,7:8) = doas;
resultat_constellation(nb_estimations,9) = P;
resultat_constellation(nb_estimations,10) = SNR;
resultat_constellation(nb_estimations,11) = nb_estimations;
resultat_constellation(nb_estimations,12:13) = phi.';
savefile = ['resultat_constellation\resultat_constellation_1_rho
           =' num2str(rho) '.mat'];
save(savefile, 'resultat_constellation');
end

% 2eme Methode : ESPRIT-ESPAR standard (sans Forward-Backward)
% -----
doas2 = doas;
A2 = [          ones(1,nsig);
      exp(sqrt(-1)*(pi/2)*cos(deg2rad*doas2));
      exp(sqrt(-1)*(pi/2)*cos(deg2rad*(doas2-60)));
      exp(sqrt(-1)*(pi/2)*cos(deg2rad*(doas2-120)));
      exp(sqrt(-1)*(pi/2)*cos(deg2rad*(doas2-180)));
      exp(sqrt(-1)*(pi/2)*cos(deg2rad*(doas2-240)));
      exp(sqrt(-1)*(pi/2)*cos(deg2rad*(doas2-300)))
];

x2 = ((W*A2)*sig) + noise;
[doae2, doa2, ags2, phi2] = esprit_sans_fb(x2, P, M, J1, J2, pa, W,
K, J, doas2);
if length(find(imag(doe2))) == 0
    sum_angle2 = sum_angle2 + sort(doe2.'');
    sum_erreur2 = sum_erreur2 + abs(sort(doe2.'')-(doas2));
    nb_estimations2 = nb_estimations2 + 1;
    tab_estimation2(nb_estimations2,:) = [doae2.' doa2.' ags2];
    % enregistrement des resultats
    resultat_constellation2(nb_estimations2,1) = rho;
    resultat_constellation2(nb_estimations2,2) = erho;
    resultat_constellation2(nb_estimations2,3:4) = doae2.';
    resultat_constellation2(nb_estimations2,5:6) = doa2.';
    resultat_constellation2(nb_estimations2,7:8) = doas;
    resultat_constellation2(nb_estimations2,9) = P;
    resultat_constellation2(nb_estimations2,10) = SNR;
    resultat_constellation2(nb_estimations2,11) = nb_estimations2;
    resultat_constellation2(nb_estimations2,12:13) = phi2.';
    savefile = ['resultat_constellation\resultat_constellation2_1_rho
               =' num2str(rho) '.mat'];

```

```

        save(savefile, 'resultat_constellation2');
    end

    % partie affichage graphique
    th=0:pi/100:pi*2;
    th1 = 0:pi/100:2*pi;
    figure(nb_mesures)
    plot(real(doa),imag(doa),'rx','LineWidth',2);
    plot(cos(th1),sin(th1),'b--');
    hold on;
    axis([-1.5 1.5 -1.5 1.5]);
    axis image;
    figure(nb_mesures+1)
    plot(real(doa2),imag(doa2),'b+','LineWidth',2);
    plot(cos(th1),sin(th1),'b--');
    hold on;

    % Affichage graphique
    % th=0:pi/100:pi*2;
    % th1 = 0:pi/100:2*pi;
    % figure(nb_mesures)
    % plot(real(doa),imag(doa),'rx',real(ags),imag(ags),'ko','LineWidth',
    % 4);
    % hold on
    % plot(real(doa2),imag(doa2),'b+',real(ags2),imag(ags2),'ko',
    % 'LineWidth',4);
    % plot(cos(th1),sin(th1),'b--');
    %hold off;

    %   texte1 = ['\theta_'];
    %   for index=1:nsig
    %       texte1=[texte1 num2str(index) '=' num2str(doas(index)) 'ř';
    % estimate' num2str(index) '= ' num2str(doae(index),'%3.2f') 'ř;'];
    %       if (index~=nsig)
    %           texte1 = [ texte1 '\newline\theta_'];
    %       end
    %   end
    %
    %   text(-0.6,0.4,texte1,'FontWeight','Bold','FontSize',16,
    % 'FontName','Times');
    %h=legend('Estimated with fb', 'DoA','Estimated without fb',0);
    %set(h,'FontWeight','Bold','FontSize',16,'FontName','Times',

```

```

    % 'LineWidth',1);
    h = get(gcf,'CurrentAxes');
    set(h,'FontWeight','Bold','FontSize',16,'FontName','Times',
        'LineWidth',1);
    %texte1 = ['\rho = ', num2str(rho)];
    %text(-0.3,0,texte1,'FontWeight','Bold','FontSize',16,'FontName',
    % 'Times');
    axis([-1 1 0 1]);
    axis image;
    %hold off;
    grid off

end
mean_angle = sum_angle/nb_estimations;
mean_angle2 = sum_angle2/nb_estimations2;
% calcul de l'erreur moyenne d'estimation
erreur_angle = sum_erreur/nb_estimations;
erreur_angle2 = sum_erreur2/nb_estimations2;
% enregistrement des resultats
resultat(nb_mesures, 1) = SNR;
resultat(nb_mesures, 2:3) = mean_angle;
resultat(nb_mesures, 4:5) = mean_angle2;
resultat(nb_mesures, 6) = NB_ITERATIONS;
resultat(nb_mesures, 7) = rho;
resultat(nb_mesures, 8) = erho;
resultat(nb_mesures, 9) = P;
resultat(nb_mesures, 10:11) = doas;
resultat(nb_mesures, 12) = nb_estimations;
resultat(nb_mesures, 13) = nb_estimations2;
resultat(nb_mesures, 14:15) = erreur_angle;
resultat(nb_mesures, 16:17) = erreur_angle2;
resultat(nb_mesures, 18) = doas(2)-doas(1);
savefile = 'resultat_rho_fb_1.mat';
save(savefile, 'resultat');

% Deux facon d'incrementer rho
rho = (rho+1)/2;
%rho = rho + pas_incrementation;
end
hold off;

figure(nb_mesures+1);
plot(resultat(:,7), resultat(:,14), 'r','LineWidth',2);

```

```

hold on;
plot(resultat(:,7), resultat(:,15), 'b','LineWidth',2);
plot(resultat(:,7), resultat(:,16), 'r--','LineWidth',2);
plot(resultat(:,7), resultat(:,17), 'b--','LineWidth',2);
xlabel('correlation coefficient \rho','FontWeight','Bold','FontSize',12,
'FontName','Times');
ylabel('Estimation Error (degree)','FontWeight','Bold','FontSize',12,
'FontName','Times');
h=legend('FBA-ESPRIT - signal 1','FBA-ESPRIT - signal 2','ESPRIT - signal 1',
'ESPRIT - signal 2',0);
set(h,'FontWeight','Bold','FontSize',16,'FontName','Times','LineWidth',1);
%axis([0.75 1 0 55]);
grid on;
nom_fich = ['fig_rho_fb_1.eps'];
print('-depsc', nom_fich);
nom_fich = ['fig_rho_fb_1.jpg'];
print('-djpeg', nom_fich);

duree_simulation = etime(clock, tps)      % duree de la simulation

```

## esprit\_var\_SNR.m

<pre>program name: esprit_var_SNR.m comments: Investigation of the influence of the angular distance between signals</pre>
--

```
%
% Teste l'influence de la valeur du SNR (Signal to Noise Ratio) sur la
% performance d'estimation des DoAs en employant ESPRIT pour ESPAR et
% FBA-ESPRIT pour ESPAR
%
clear all;
clf;
close all;

tps = clock;          % horloge au debut de la simulation

P = 10000;           % Number of snapshot to define a signal
doas = [35 145];     % DoAs of signals
NB_ITERATIONS = 2000; % Number of trials
rho = 0.0;           % correlation coefficient of the two signals
alpha1 = 0.0000000000001; % Couronne de validite autour du cercle unite
% pour le critere de validite
M = 7;               % Number of elements of the ESPAR antenna
x0 = 50;

rad2deg = 180/pi;
deg2rad = pi/180;

e11 = [1 0 0 0].';
e12 = [0 1 0 0].';
e13 = [0 0 1 0].';
e14 = [0 0 0 1].';
zer = [0 0 0 0].';

J = fliplr(diag(ones(1,M)));

react = [ 0 0 0 0 0 0 ;
          300 300 -300 -300 -300 300;
          300 300 300 -300 -300 -300;
          -300 300 300 300 -300 -300;
          -300 -300 300 300 300 -300;
```



```

-300 -300 -300 300 300 300;
300 -300 -300 -300 300 300
];

y00 = 0.00023344-j*0.0066918;
y10 = -0.0001816+j*0.00242469;
y11 = 0.00300676-j*0.0044176;
y21 = 0.00097427+j*0.00299986;
y31 = -0.0003066-j*0.0003067;
y41 = 0.0000973-j*0.0001353;

Y = [y00 y10 y10 y10 y10 y10 y10;
      y10 y11 y21 y31 y41 y31 y21;
      y10 y21 y11 y21 y31 y41 y31;
      y10 y31 y21 y11 y21 y31 y41;
      y10 y41 y31 y21 y11 y21 y31;
      y10 y31 y41 y31 y21 y11 y21;
      y10 y21 y31 y41 y31 y21 y11];

Z = inv(Y);
u0 = [1 0 0 0 0 0 0].';

zs = 50;

% Calculate the weight matrix W
W = zeros(M,M);
for index= 1:M
    W(index,:) = (2*zs*inv(Z+diag([zs;j*react(index,:).']))) * u0).';
end

nb_mesures = 0; % initialisation du nombre de mesures
               % (1 mesure = 1 valeur du SNR particuliere)

for SNR=30:-1:-15
    nb_mesures = nb_mesures + 1
    mean_angle = 0; % valeur moyenne des angles estimes avec la 1ere
                   % methode (FBA-ESPRIT-ESPAR)
    mean_angle2 = 0; % valeur moyenne des angles estimes avec la 2eme
                    % methode (ESPRIT-ESPAR)
    sum_angle(1:2) = 0; % Somme des angles estime avec la 1ere methode
    sum_angle2(1:2) = 0; % Somme des angles estime avec la 2eme methode
    sum_erreur(1:2) = 0;
    sum_erreur2(1:2) = 0;
    nb_estimations = 0; % nombre de signaux estimes avec la 1ere methode

```

```

nb_estimations2 = 0; % nombre de signaux estimes avec la 2eme methode
clear resultat_constellation;
clear resultat_constellation2;
for indice_iteration = 1 : NB_ITERATIONS
    J1 = [e13, e11, e12, zer, zer, zer, e14]; % Matrice de selection J1
    J2 = [e11, zer, zer, e12, e13, e14, zer]; % Matrice de selection J2
    K = [J1;J2];
    [symbols, erho, ecov] = creer_2sigcorr(P, rho);
    nsig = length(doas);
    noise = randn(7,P) + sqrt(-1)*randn(7,P);

    [nsig,P] = size(symbols);

% 1ere Methode : Forward-Backward combine avec ESPRIT
% -----
A = [
        ones(1,nsig);
        exp(sqrt(-1)*(pi/2)*cos(deg2rad*doas));
        exp(sqrt(-1)*(pi/2)*cos(deg2rad*(doas-60)));
        exp(sqrt(-1)*(pi/2)*cos(deg2rad*(doas-120)));
        exp(sqrt(-1)*(pi/2)*cos(deg2rad*(doas-180)));
        exp(sqrt(-1)*(pi/2)*cos(deg2rad*(doas-240)));
        exp(sqrt(-1)*(pi/2)*cos(deg2rad*(doas-300)))
];

psym = diag((symbols*symbols')/P);

% Tous les signaux ont le meme SNR
sig = diag(sqrt((2*(10.^(SNR/10.0)))./psym)) * symbols;
x = ((W*A)*sig) + noise;
pa=nsig;
[doae, doa, ags, phi] = esprit_avec_fb(x, P, M, J1, J2, pa, W, K,
J, doas);
if length(find((1-alpha1)<=abs(phi) & abs(phi)<=(1+alpha1))) == nsig
    sum_angle = sum_angle + sort(doa);
    sum_erreur = sum_erreur + abs(sort(doa)-sort(doas));
    nb_estimations = nb_estimations + 1;
    tab_estimation(nb_estimations,:) = [doae.' doa.' ags];
    % enregistrement des resultats
    resultat_constellation(nb_estimations,1) = rho;
    resultat_constellation(nb_estimations,2) = erho;
    resultat_constellation(nb_estimations,3:4) = doae.';
    resultat_constellation(nb_estimations,5:6) = doa.';
    resultat_constellation(nb_estimations,7:8) = doas;

```

```

resultat_constellation(nb_estimations,9) = P;
resultat_constellation(nb_estimations,10) = SNR;
resultat_constellation(nb_estimations,11) = nb_estimations;
resultat_constellation(nb_estimations,12:13) = phi.';
savefile = ['resultat_constellation\resultat_constellation_1_snr
            =' num2str(abs(diff(doas))) '.mat'];
save(savefile, 'resultat_constellation');
end

% 2eme Methode : ESPRIT standard (sans Forward-Backward)
% -----
doas2 = doas;
A2 = [
        ones(1,nsig);
        exp(sqrt(-1)*(pi/2)*cos(deg2rad*doas2));
        exp(sqrt(-1)*(pi/2)*cos(deg2rad*(doas2-60)));
        exp(sqrt(-1)*(pi/2)*cos(deg2rad*(doas2-120)));
        exp(sqrt(-1)*(pi/2)*cos(deg2rad*(doas2-180)));
        exp(sqrt(-1)*(pi/2)*cos(deg2rad*(doas2-240)));
        exp(sqrt(-1)*(pi/2)*cos(deg2rad*(doas2-300)))
];

x2 = ((W*A2)*sig) + noise;
[doae2, doa2, ags2, phi2] = esprit_sans_fb(x2, P, M, J1, J2, pa, W,
K, J, doas2);
if length(find(imag(doe2))) == 0
    sum_angle2 = sum_angle2 + sort(doe2. ');
    sum_erreur2 = sum_erreur2 + abs(sort(doe2. ')-(doas2));
    nb_estimations2 = nb_estimations2 + 1;
    tab_estimation2(nb_estimations2,:) = [doae2.' doa2.' ags2];
    % enregistrement des resultats
    resultat_constellation2(nb_estimations2,1) = rho;
    resultat_constellation2(nb_estimations2,2) = erho;
    resultat_constellation2(nb_estimations2,3:4) = doae2.';
    resultat_constellation2(nb_estimations2,5:6) = doa2.';
    resultat_constellation2(nb_estimations2,7:8) = doas;
    resultat_constellation2(nb_estimations2,9) = P;
    resultat_constellation2(nb_estimations2,10) = SNR;
    resultat_constellation2(nb_estimations2,11) = nb_estimations2;
    resultat_constellation2(nb_estimations2,12:13) = phi2.';
    savefile = ['resultat_constellation\resultat_constellation2_5_snr
                =' num2str(abs(diff(doas))) '.mat'];
    save(savefile, 'resultat_constellation2');
end

```

```

% partie affichage graphique
% th=0:pi/100:pi*2;
% th1 = 0:pi/100:2*pi;
% figure(nb_mesures)
% plot(real(doa),imag(doa),'rx',real(ags),imag(ags),'ko','LineWidth',
% 4);
% hold on
% plot(real(doa2),imag(doa2),'bx',real(ags2),imag(ags2),'ko',
% 'LineWidth',4);
% plot(cos(th1),sin(th1),'b--');
% hold off;
%
% texte1 = ['\theta_'];
% for index=1:nsig
% texte1=[texte1 num2str(index)']='num2str(doa(index))'ř;
% estimate' num2str(index)']='num2str(doa(index),'%3.2f')'ř;'];
% if (index~=nsig)
% texte1 = [ texte1 '\newline\theta_'];
% end
% end
%
% text(-0.6,0.4,texte1,'FontWeight','Bold','FontSize',16,
% 'FontName','Times');
%
% h=legend('Estimated with fb', 'DoA','Estimated without fb',0);
% set(h,'FontWeight','Bold','FontSize',16,'FontName','Times',
% 'LineWidth',1);
% h = get(gcf,'CurrentAxes');
% set(h,'FontWeight','Bold','FontSize',16,'FontName','Times',
% 'LineWidth',1);
% texte1 = ['\rho = ', num2str(rho)];
% text(-0.3,0,texte1,'FontWeight','Bold','FontSize',16,'FontName',
% 'Times');
% axis([-1 1 0 1]);
% axis image;
% hold off;
% grid off

end
mean_angle = sum_angle/nb_estimations;
mean_angle2 = sum_angle2/nb_estimations2;

```

```

% calcul de l'erreur moyenne d'estimation
erreur_angle = sum_erreur/nb_estimations;
erreur_angle2 = sum_erreur2/nb_estimations2;
% enregistrement des resultats
resultat(nb_mesures, 1) = SNR;
resultat(nb_mesures, 2:3) = mean_angle;
resultat(nb_mesures, 4:5) = mean_angle2;
resultat(nb_mesures, 6) = NB_ITERATIONS;
resultat(nb_mesures, 7) = rho;
resultat(nb_mesures, 8) = erho;
resultat(nb_mesures, 9) = P;
resultat(nb_mesures, 10:11) = doas;
resultat(nb_mesures, 12) = nb_estimations;
resultat(nb_mesures, 13) = nb_estimations2;
resultat(nb_mesures, 14:15) = erreur_angle;
resultat(nb_mesures, 16:17) = erreur_angle2;
resultat(nb_mesures, 18) = doas(2)-doas(1);
savefile = 'resultat_snr_fb_1.mat';
save(savefile, 'resultat');

end
hold off;

% disp(['Estimations bonnes : ' num2str(nbEstimBon)]);
% disp(['Estimations mauvaises : ' num2str(nbEstimMauvais)]);
% disp(['Moyenne des DoA estime : ' num2str(MoyenneDoA.)]);

figure(nb_mesures+1);
plot(resultat(:,1), resultat(:,14), 'r','LineWidth',2);
hold on;
plot(resultat(:,1), resultat(:,15), 'b','LineWidth',2);
plot(resultat(:,1), resultat(:,16), 'r--','LineWidth',2);
plot(resultat(:,1), resultat(:,17), 'b--','LineWidth',2);
xlabel('SNR (dB)', 'FontWeight', 'Bold', 'FontSize', 12, 'FontName', 'Times');
ylabel('Estimation Error (degree)', 'FontWeight', 'Bold', 'FontSize', 12,
'FontName', 'Times');
h=legend('FBA-ESPRIT - signal 1', 'FBA-ESPRIT - signal 2', 'ESPRIT - signal 1'
, 'ESPRIT - signal 2', 0);
set(h, 'FontWeight', 'Bold', 'FontSize', 16, 'FontName', 'Times', 'LineWidth', 1);
% axis([0 50 0 45]);
grid on;
nom_fich = ['fig_snr_fb_1.eps'];
print('-depsc', nom_fich);
nom_fich = ['fig_snr_fb_1.jpg'];

```

```
print('-djpeg', nom_fich);
```

```
duree_simulation = etime(clock, tps)           % duree de la simulation
```

## esprit\_var\_angle.m

<pre>program name: esprit_var_angle.m comments: Investigation of the influence of the angular distance between signals</pre>
--

```
%
% Teste l'influence de la distance angulaire entre 2 signaux
% sur la performance d'estimation des DoAs en employant
% ESPRIT pour ESPAR et FBA-ESPRIT pour ESPAR
%

clear all;
clf;
close all;

tps = clock;           % horloge au debut de la simulation

P = 10000;             % Number of snapshot to define a signal
SNR = 25;              % Signal to Noise Ratio (dB)
doas = [-1 181];       % DoAs of signals
NB_ITERATIONS = 2000; % Number of trials
rho = 0.95;            % correlation coefficient of the two signals
alpha1 = 0.000000000001; % Couronne de validite autour du cercle unite
                                % pour le critere de validite
M = 7;                 % Number of elements of the ESPAR antenna
x0 = 50;

rad2deg = 180/pi;
deg2rad = pi/180;

e11 = [1 0 0 0].';
e12 = [0 1 0 0].';
e13 = [0 0 1 0].';
e14 = [0 0 0 1].';
zer = [0 0 0 0].';

J = fliplr(diag(ones(1,M)));

react = [ 0 0 0 0 0 0 ;
         300 300 -300 -300 -300 300;
         300 300 300 -300 -300 -300;
         -300 300 300 300 -300 -300;
```

```

-300 -300 300 300 300 -300;
-300 -300 -300 300 300 300;
300 -300 -300 -300 300 300
];

y00 = 0.00023344-j*0.0066918;
y10 = -0.0001816+j*0.00242469;
y11 = 0.00300676-j*0.0044176;
y21 = 0.00097427+j*0.00299986;
y31 = -0.0003066-j*0.0003067;
y41 = 0.0000973-j*0.0001353;

Y = [y00 y10 y10 y10 y10 y10 y10;
      y10 y11 y21 y31 y41 y31 y21;
      y10 y21 y11 y21 y31 y41 y31;
      y10 y31 y21 y11 y21 y31 y41;
      y10 y41 y31 y21 y11 y21 y31;
      y10 y31 y41 y31 y21 y11 y21;
      y10 y21 y31 y41 y31 y21 y11];

Z = inv(Y);
u0 = [1 0 0 0 0 0 0].';

zs = 50;

% Calculate the weight matrix W
W = zeros(M,M);
for index= 1:M
    W(index,:) = (2*zs*inv(Z+diag([zs;j*react(index,:).']))*u0).';
end

nb_mesures = 0;    % initialisation du nombre de mesures
                  % (1 mesure = une valeur de la distance angulaire)

while ((doas(2)-doas(1)) > 0)
    doas(1) = doas(1)+1;
    doas(2) = doas(2)-1;
    nb_mesures = nb_mesures + 1
    % reinitialisation des variables
    mean_angle = 0;    % valeur moyenne des angles estimes avec la 1ere
                      % methode (FBA-ESPRIT-ESPAR)
    mean_angle2 = 0;   % valeur moyenne des angles estimes avec la
                      % 2eme methode (ESPRIT-ESPAR)

```



```

sum_angle(1:2) = 0; % Somme des angles estimes avec la 1ere methode
sum_angle2(1:2) = 0; % Somme des angles estimes avec la 2eme methode
sum_erreur(1:2) = 0;
sum_erreur2(1:2) = 0;
nb_estimations = 0; % nombre de signaux estimes avec la 1ere methode
nb_estimations2 = 0; % nombre de signaux estimes avec la 2eme methode

clear resultat_constellation;
clear resultat_constellation2;
for indice_iteration = 1 : NB_ITERATIONS
    J1 = [el3, el1, el2, zer, zer, zer, el4]; % Matrice de selection J1
    J2 = [el1, zer, zer, el2, el3, el4, zer]; % Matrice de selection J2
    K = [J1;J2];
    [symbols, erho, ecov] = creer_2sigcorr(P, rho);
    nsig = length(doas);
    noise = randn(7,P) + sqrt(-1)*randn(7,P);
    [nsig,P] = size(symbols);

    % 1ere Methode : Forward-Backward combine avec ESPRIT-ESPAR
    % -----
    A = [
        ones(1,nsig);
        exp(sqrt(-1)*(pi/2)*cos(deg2rad*doas));
        exp(sqrt(-1)*(pi/2)*cos(deg2rad*(doas-60)));
        exp(sqrt(-1)*(pi/2)*cos(deg2rad*(doas-120)));
        exp(sqrt(-1)*(pi/2)*cos(deg2rad*(doas-180)));
        exp(sqrt(-1)*(pi/2)*cos(deg2rad*(doas-240)));
        exp(sqrt(-1)*(pi/2)*cos(deg2rad*(doas-300)))
    ];

    psym = diag((symbols*symbols')/P);

    % Tous les signaux ont le meme SNR
    sig = diag(sqrt((2*(10.^(SNR/10.0)))./psym)) * symbols;
    x = ((W*A)*sig) + noise;
    pa=nsig;
    [doae, doa, ags, phi] = esprit_avec_fb(x, P, M, J1, J2, pa, W, K,
    J, doas);
    if length(find((1-alpha1)<=abs(phi) & abs(phi)<=(1+alpha1))) == nsig
        sum_angle = sum_angle + sort(doa);
        sum_erreur = sum_erreur + abs(sort(doa)-sort(doa));
        nb_estimations = nb_estimations + 1;
        tab_estimation(nb_estimations,:) = [doae.' doa.' ags];
        % enregistrement des resultats

```

```

resultat_constellation(nb_estimations,1) = rho;
resultat_constellation(nb_estimations,2) = erho;
resultat_constellation(nb_estimations,3:4) = doae.';
resultat_constellation(nb_estimations,5:6) = doa.';
resultat_constellation(nb_estimations,7:8) = doas;
resultat_constellation(nb_estimations,9) = P;
resultat_constellation(nb_estimations,10) = SNR;
resultat_constellation(nb_estimations,11) = nb_estimations;
resultat_constellation(nb_estimations,12:13) = phi.';
savefile=['resultat_constellation\resultat_constellation_1
_diffang=' num2str(abs(diff(doas))) '.mat'];
save(savefile, 'resultat_constellation');
end

% 2eme Methode : ESPRIT-ESPAR standard (sans Forward-Backward)
% -----
doas2 = doas;
A2 = [
      ones(1,nsig);
      exp(sqrt(-1)*(pi/2)*cos(deg2rad*doas2));
      exp(sqrt(-1)*(pi/2)*cos(deg2rad*(doas2-60)));
      exp(sqrt(-1)*(pi/2)*cos(deg2rad*(doas2-120)));
      exp(sqrt(-1)*(pi/2)*cos(deg2rad*(doas2-180)));
      exp(sqrt(-1)*(pi/2)*cos(deg2rad*(doas2-240)));
      exp(sqrt(-1)*(pi/2)*cos(deg2rad*(doas2-300)))
];

x2 = ((W*A2)*sig) + noise;
[doae2, doa2, ags2, phi2] = esprit_sans_fb(x2, P, M, J1, J2, pa, W,
K, J, doas2);
if length(find(imag(doe2))) == 0
    sum_angle2 = sum_angle2 + sort(doe2.'');
    sum_erreur2 = sum_erreur2 + abs(sort(doe2.'')-(doas2));
    nb_estimations2 = nb_estimations2 + 1;
    tab_estimation2(nb_estimations2,:) = [doae2.' doa2.' ags2];
% enregistrement des resultats
resultat_constellation2(nb_estimations2,1) = rho;
resultat_constellation2(nb_estimations2,2) = erho;
resultat_constellation2(nb_estimations2,3:4) = doae2.';
resultat_constellation2(nb_estimations2,5:6) = doa2.';
resultat_constellation2(nb_estimations2,7:8) = doas;
resultat_constellation2(nb_estimations2,9) = P;
resultat_constellation2(nb_estimations2,10) = SNR;
resultat_constellation2(nb_estimations2,11) = nb_estimations2;

```

```

        resultat_constellation2(nb_estimations2,12:13) = phi2.';
        savefile = ['resultat_constellation\resultat_constellation2_1
                    _diffang=' num2str(abs(diff(doas))) '.mat'];
        save(savefile, 'resultat_constellation2');
    end

% partie affichage graphique
%
% th=0:pi/100:pi*2;
% th1 = 0:pi/100:2*pi;
% figure(nb_mesures)
% plot(real(doa),imag(doa),'rx',real(ags),imag(ags),'ko','LineWidth'
%     ,4);
% hold on
% plot(real(doa2),imag(doa2),'bx',real(ags2),imag(ags2),'ko',
%     'LineWidth',4);
% plot(cos(th1),sin(th1),'b--');
% hold off;
%
%
%     texte1 = ['\theta_'];
%     for index=1:nsig
%         texte1=[texte1 num2str(index)']='num2str(doas(index))'ř;
%         estimate'num2str(index)']='num2str(doa2(index),'%3.2f')'ř;'];
%         if (index~=nsig)
%             texte1 = [ texte1 '\newline\theta_'];
%         end
%     end
%
%     text(-0.6,0.4,texte1,'FontWeight','Bold','FontSize',16,
%         'FontName','Times');
% h=legend('Estimated with fb', 'DoA','Estimated without fb',0);
% set(h,'FontWeight','Bold','FontSize',16,'FontName','Times',
%     'LineWidth',1);
% h = get(gcf,'CurrentAxes');
% set(h,'FontWeight','Bold','FontSize',16,'FontName','Times',
%     'LineWidth',1);
% texte1 = ['\rho = ', num2str(rho)];
% text(-0.3,0,texte1,'FontWeight','Bold','FontSize',16,'FontName',
%     'Times');
% axis([-1 1 0 1]);
% axis image;
% hold off;
% grid off

```

```

end
mean_angle = sum_angle/nb_estimations;
mean_angle2 = sum_angle2/nb_estimations2;
% calcul de l'erreur moyenne d'estimation
erreur_angle = sum_erreur/nb_estimations;
erreur_angle2 = sum_erreur2/nb_estimations2;
% enregistrement des resultats
resultat(nb_mesures, 1) = SNR;
resultat(nb_mesures, 2:3) = mean_angle;
resultat(nb_mesures, 4:5) = mean_angle2;
resultat(nb_mesures, 6) = NB_ITERATIONS;
resultat(nb_mesures, 7) = rho;
resultat(nb_mesures, 8) = erho;
resultat(nb_mesures, 9) = P;
resultat(nb_mesures, 10:11) = doas;
resultat(nb_mesures, 12) = nb_estimations;
resultat(nb_mesures, 13) = nb_estimations2;
resultat(nb_mesures, 14:15) = erreur_angle;
resultat(nb_mesures, 16:17) = erreur_angle2;
resultat(nb_mesures, 18) = doas(2)-doas(1);
savefile = 'resultat_ang_fb_1.mat';
save(savefile, 'resultat');

end
hold off;

figure(nb_mesures+1);
plot(resultat(:,18), resultat(:,14), 'r','LineWidth',2);
hold on;
plot(resultat(:,18), resultat(:,15), 'b','LineWidth',2);
plot(resultat(:,18), resultat(:,16), 'r--','LineWidth',2);
plot(resultat(:,18), resultat(:,17), 'b--','LineWidth',2);
xlabel('\Delta\theta (degree)', 'FontWeight', 'Bold', 'FontSize', 12, 'FontName',
    'Times');
ylabel('Estimation Error (degree)', 'FontWeight', 'Bold', 'FontSize', 12
    , 'FontName', 'Times');
h=legend('FBA-ESPRIT - signal 1', 'FBA-ESPRIT - signal 2'
    , 'ESPRIT - signal 1', 'ESPRIT - signal 2', 0);
set(h, 'FontWeight', 'Bold', 'FontSize', 16, 'FontName', 'Times', 'LineWidth', 1);
axis([0 180 0 40]);
grid on;
nom_fich = ['fig_ang_fb_1.eps'];

```

```
print('-depsc', nom_fich);  
nom_fich = ['fig_ang_fb_1.jpg'];  
print('-djpeg', nom_fich);  
  
duree_simulation = etime(clock, tps)    % duree de la simulation
```

